INTERPRETATION OF RESISTIVITY SOUNDINGS FROM SAN IGNACIO, HONDURAS

Orlando Pena Ruíz

Geothermal Training Programme
Reykjavík, Iceland
Report 6, 1988

Report 6, 1988

INTERPRETATION OF RESISTIVITY SOUNDINGS FROM SAN IGNACIO, HONDURAS

Orlando Pena Ruíz
UNU Geothermal Training Programme
National Energy Authority
Grensásvegur 9
108 Reykjavík
ICELAND

Permanent Address:
Empresa Nacional de Energia Eléctrica
Division de Ingeniería Civil
P.O. Box 99 Tegucigalpa,D.C.
HONDURAS

ABSTRACT

The San Ignacio geothermal field is located in the central part of Honduras. The rocks in the area are primarily of Paleozoic metamorphic origin, overlaid by Tertiary Padre Miguel Group tuffs and alluvial deposits. One-dimensional interpretation of Schlumberger resistivity soundings revealed that the alluvial deposits have a relatively low resistivity and hence obscured possible interesting resistivity structure in the underlaying basement. The geothermal surface manifestations are located where a NE-trending zone of most recent tectonic activity, west of the Arenal-fault, intersects a WNW-trending fault bordering the northern part of the Siria valley. A low-resistivity anomaly is present in the southwest extension of the zone, covering an area of 15 km^2. All this together with the presence of the sinter deposits north of La Tembladera might suggest that the geothermal activity is related to this NE-trending fault zone and the low resistivity could be caused by geothermal fluids conducted by these faults and infiltrated into the valley fill.

TABLE OF CONTENTS

LIST OF FIGURES

1. INTRODUCTION

1.1 Scope of Work

In this report the author presents the results of the work carried out during 6 months at the **UNU** Geothermal Training Programme in Iceland in 1988.

The training programme started with 5 weeks of introductory lectures. They were followed by an introduction to the theory of DC-resistivity soundings and the resistivity of rocks. Practical training in geophysical exploration was included in the programme with special emphasis on geoelectrical methods, such as Schlumberger soundings and head-on profiling.

To get acquainted with the practical applications of the geoelectrical methods, the author was in a field-crew participating in performing Schlumberger soundings and head-on profiling.

The main research project of the author was the interpretation of 81 Schlumberger soundings from the San Ignacio geothermal field in Honduras. These soundings were analyzed and interpreted with a one-dimensional inversion program using the PC-computer facilities at the **UNU**. Resistivity cross-sections and iso-resistivity maps were made in order to understand the resistivity structure of the area. The results were compared with the tectonics and other geological features of the area as well as gravimetric and magnetic results, leading to an integrated model of the geothermal field.

The author also participated in a magnetic survey,carried out for locating a borehole and a magnetotelluric survey, whose purpose was to map resistivity structure at great depths.

1.2 Resistivity Survey in Geothermal Exploration

Almost all geophysical methods have been used for exploring various types of geothermal systems. The success of a geophysical method detecting a particular physical parameter depends upon the contrast of that parameter inside and outside of a geothermal system giving rise to certain geophysical anomalies. Resistivity surveys are of particular importance in mapping temperature anomalies, faults, fractures, lithological contacts, thermal brine, and zones of hydrothermal alteration. Thermal waters become increasingly conductive with increasing salinity and with increasing temperature up 300°C above which conductivity slightly decreases.

According to Hochstein (1980), resistivity surveys used for geothermal prospecting can be broadly grouped into:

- Reconnaissance mapping (also called profiling or traversing). It is usually the first type of survey made to determine the gross resistivity features of geothermal prospects.

- Vertical electrical sounding (VES). It involves a survey to determine the vertical resistivity structure.

- Location of steep boundaries. It involves a follow-up to define the boundaries and boundary structure of geothermal reservoirs.

The aim of resistivity soundings is to get information on the electrical properties of the earth which can reflect the strata at different depths. Resistivity is directly related to parameters like salinity, temperature and porosity, parameters that characterize the reservoir to a great extent. The physical relevance of resistivity, its geothermal importance, is discussed in chapter 2. The next task is to show how to arrive at the resistivity of the earth. Resistivity is defined through Ohm's law i.e.:

$$\mathbf{E} = \rho \mathbf{j}$$

Where **E** (V/m) is the electric field and **j** (A/m^2) is the current density. By introducing a known current into the earth and measure the corresponding electric field (potential difference between two closely spaced points, $E = \Delta V/L$), one can get an information on the resistivity structure of the subsurface.

Various techniques have been used depending on the information needed. The most common electrode configuration is the Schlumberger array. Other configurations include the head-on profiling, the equatorial dipole and to a smaller extent the quadrupole, Wenner and coaxial dipole configuration. In chapter 3 two of these will be discussed i.e. Schlumberger soundings and head-on profiling, both theory and field procedure. The interpretation of Schlumberger soundings is the task of chapter 4, while the instrumentation is described in chapter 5. The usefulness of resistivity soundings is demonstrated in chapter 6.

2. THE ELECTRICAL RESISTIVITY OF ROCKS

2.1 Introduction

Of all the geophysical methods that have been used to prospect for geothermal reservoir particularly in areas where hot water fields dominate, those which measure the electrical resistivity at depth in the ground have been the most useful (Lumb, 1980). One of the main reasons for this success is that the resistivity variations observed are related directly to properties of the actual object of the search (hot water) and not only to the host rocks. Thus resistivity maps can indicate the areal extent of a hot water reservoir over whatever depth range the survey technique is able to probe.

The resistivity of a body of rock containing an electrolyte depends on the resistivity of the electrolyte and the temperature and to a lesser extent on the resistivity of the rock itself. The measured resistivity also depends on the porosity and the extent to which the voids are filled with electrolyte. In a geothermal field the electrolyte involved is the geothermal fluid and its resistivity is inversely related to the concentration of ions that it carries. The temperature dependance of the resistivity decreases with increasing temperature (Keller and Frischknecht, 1966) and according to Risk et al. (1970) changes due to variations in porosity dominate above 150°C.

Electrical conductivity of a matter (σ) describes the ability of that matter to conduct electrical current. The reciprocal of conductivity is resistivity (ρ). It describes the ability to resist an electrical current. Resistivity has the unity Ωm. Resistivity of a matter is defined as the ratio of potential difference (ΔV) to current (I) across material which has a cross-sectional area (A) of 1 m^2 and is 1 m length (L).

$$\rho = \frac{\Delta V}{I} \frac{A}{L}$$

Table 1 shows typical electrical resistivity of Icelandic rocks.

Formation	Resistivity (Ωm)
Recent lava flow	5.000-50.000
Dense intrusives	10.000-15.000
Basalt	100-300
Palagonite	20-100
Basalt (T>50°C)	30-100
Palagonite (T>50°C)	10-15
Rocks with brine	5-15
High temperature areas, fresh water	1-5
High temperature areas, brine areas	1-4

TABLE 1. Electrical resistivity of Icelandic rocks

As already mentioned in the beginning of this chapter the electrical resistivity depends on:

-Amount of water (saturation)
-Pressure
-Salinity of the water
-Temperature of the water
-Pore structure of the rock
-Alteration

2.2 Resistivity Versus Water Content and Pressure

In geothermal areas the rocks are water saturated. Ionic conduction in the saturated fluid depends on the number and mobility of ions and the connectivity of flow paths through the rock matrix. Usually the saturating fluid is among the dominant conductor in the rock and the degree of saturation is of great importance to the bulk resistivity.

Resistivity of water increases about one order of magnitude because of the lithostatic pressure down through the earth's crust. Thus the pressure dependance is neglible to the temperature dependance provided that the pressure is sufficiently high so that there is no change in phase.

2.3 Resistivity Versus Salinity

Salinity of electrolytes, such as NaCl in water, affects resistivity in nearly inversely linear manner (Keller and Frischknecht 1966). At T=0°C we have:

$$\rho = 9.545\ C^{-0.937} = 10/C$$

Where C (g/l) is the concentration of NaCl.

2.4 Resistivity Versus Temperature

For temperatures upto 150-200°C the resistivity of the pore fluid decreases with increasing temperature. The dominant factor is increasing mobility of ions caused by lower viscosity of the water. Dakhnov (1962) has described this relation:

$$\rho_w = \frac{\rho_{wo}}{1+\alpha(T-T_o)}$$

Where:

ρ_{wo} : resistivity of the fluid at temperature T_o
α : temperature coefficient of resistivity, $\alpha = 0.023\ C^{-1}$ for T_o=23°C, and 0.025 for T_o=0°C.

Figure 1 shows the resistivity of NaCl solutions as a function of temperature. It also shows how resistivity depends on the concentration of the electrolyte. The concentrations are typical of geothermal brines (Ucok, 1979).

At high temperatures a decrease in the dielectric permittivity of the water results in a decrease in the number of dissociated ions in solution. Above 300°C this starts to increase fluid resistivity (Quist and Marshall, 1968).

2.5 Resistivity Versus Porosity

Porosity is defined as the ratio between the pore volume and the total volume of a material. There are mainly three types of porosity.

- Intergranular: The pores are formed as space between grains or particles in a compact material. Example: Sediments.

- Joints: A net of fine fractures caused by tension and cooling of the rock. Example: Lava.

- Vugular porosity: Big and irregular pores, formed as materials are dissolved and washed away or pores formed by gas (lava).

Archie's law describes how resistivity depends on porosity if ionic conduction in the pore fluid dominates other conduction mechanism in the rocks (Archie, 1942). It is valid if the resistivity of the pore fluid is of the order of 1 Ωm or less, but doubts are raised if the resistivity is much higher (Duba et al., 1978).

$$\rho = \rho_w . a\phi_t^{-n}$$

Where:

ρ : bulk resistivity
ρ_w: resistivity of pore fluid
ϕ_t: porosity
a : empirical parameter, varies from less than 1 for intergranular porosity to over 1 for joint porosity, usually around 1

n : an cementation factor, an empirical parameter, varies from 1.2 for unconsolidated sediments to 3.5 for crystalline rocks, usually around 2

Figure 2 shows the bulk resistivity as a function of the total porosity for samples taken in Iceland at 500 m depth (Flóvenz et al., 1985). The resistivity has been corrected for variable temperature and refers to T = 23°C.

2.6 Resistivity Versus Alteration

Water-rock interaction results in an alteration of the rock matrix. The type of alteration minerals formed is dependent upon the temperature and the chemical composition of the fresh rocks and the saturating fluid. Results from Nesjavellir high-temperature area in Iceland show the following correlation between temperature, alteration and resistivity (Árnason and Hersir, 1988). At temperatures below 200°C clay minerals are dominant but chlorite and epidote above 250°C. Between 200°C and 250°C there is a transition, called mixed-layer. Clay minerals are well-conducting and can dominate the conductivity of the saturated rock, but chlorite and epidote are resistive.

3. THE THEORY OF DC-RESISTIVITY SOUNDINGS

3.1 Schlumberger Soundings

The Schlumberger configuration shown in Figure 3a is used to determine the apparent resistivity. In the Schlumberger array two potential and two current electrodes are placed along a straight line, the array being symmetrical around the middle point, O. Current electrodes are placed at A and B and potential electrodes are placed at M and N. The distance between the potential electrodes MN, 2P, is kept much smaller than the distance between the current electrodes AB, 2S (at least five times smaller). We will see how the Schlumberger array gives the resistivity of a homogeneous earth in terms of the injected current and the measured potential difference between the potential electrodes. The resulting formula will be used to define the term apparent resistivity for a non-homogeneous earth.

At the surface of a homogeneous and isotropic earth the potential at a point at the distance r from a point of current injection is given as:

$$V(r) = \frac{\rho I}{2\pi r}$$

Where :

V : the potential
ρ : the resistivity
I : the current strength
r : the distance from the current source to the measuring point.

For distances marked as in Figure 3a and the current I transmitted to the ground at A (-I at B) the potential at N will be:

$$V_N = V_N(A) + V_N(B) = \frac{\rho I}{2\pi(S+P)} + \frac{\rho(-I)}{2\pi(S-P)}$$

$$= \frac{\rho I}{2\pi}\left(\frac{1}{S+P} - \frac{1}{S-P}\right)$$

The potential at M is:

$$V_M = V_M(A) + V_M(B) = \frac{\rho I}{2\pi(S-P)} + \frac{\rho(-I)}{2\pi(S+P)}$$

$$= \frac{\rho I}{2\pi}\left(\frac{1}{S-P} - \frac{1}{S+P}\right)$$

The potential difference becomes:

$$\Delta V = V_M - V_N = \frac{\rho I}{2\pi} 2\left(\frac{1}{S-P} - \frac{1}{S+P}\right) = \frac{2\rho IP}{\pi(S^2-P^2)}$$

This equation can be solved for ρ and which can thus be calculated from the measured transmitted current and the corresponding measured potential. The resistivity for a homogeneous earth becomes:

$$\rho = \frac{\pi(S^2-P^2)\Delta V}{2PI}$$

If the earth is not homogeneous the resistivity which is calculated from the measured values of the current and the potential is defined as the apparent resistivity, ρa i.e. the resistivity a homogeneous earth would actually have to give those particular measured values for the current and the potential.

Therefore the apparent resistivity is given by:

$$\rho_a = \frac{\Delta V}{I} \cdot \frac{\pi(S^2-P^2)}{2P}$$

3.1.1 Field procedure

In resistivity surveys the field procedure depends on the type of electrode configuration used. In the Schlumberger array four electrodes are symmetrically positioned along a straight line (see Figure 3a). The distance between current electrodes (AB) is considerably larger than that of the potential electrodes (MN). The distance between the current electrodes is increased in certain steps and measurements are made for each point. The distance between the current electrodes is increased exponentially usually with 10 point per decade. In Iceland the starting length of half the current electrode spacing (AB/2) is usually 2.51 or 10 m, and the maximum spacing is usually 1780 m, sometimes as high as 3000 m. As the current electrode spacing increases the potential signal decreases. Therefore half the potential electrode spacing (MN/2) is increased in steps, from 1 to 100 m.

By increasing the current electrode spacing, the current penetrates deeper into the earth and information is received on resistivity at greater depths. When the apparent resistivity has been calculated it is plotted as a function of half the current electrode spacing on a log-log paper and is ready for interpretation.

It takes 4 people to carry out a Schlumberger sounding. One controls the instruments. One writes down the results and plots the apparent resistivity curve. Two people move the current electrodes, one in each direction. At each point they push the electrodes into the ground and connect them to the transmitter cable, step back and announce in a portable walkie-talkie that all is set. Then the measurement at that point takes place. At the end of the sounding, a check for current leakage is made, one current electrode is disconnected, then a high voltage is put on the transmitter cable and the potential between M and N measured as well as the transmitted current. This is made for both electrodes.

If the measured potential signal is about 10% of the signal obtained when both current electrodes are connected or higher, something is wrong and has to be mended.

3.2 Head-on Profiling

Schlumberger soundings are useful in pointing out areas of low resistivity. They can be used to compare different areas and together with thermal gradient measurements they may be helpful in selecting promising fields for further investigation. The resolution of the Schlumberger soundings is, however, too limited to detect and map a single waterbearing dike or fracture. The prospecting method which seems to be the most powerful one in locating permeable, near vertical structures is the so called head-on resistivity profiling (Cheng 1980; Flóvenz 1984). The set-up is shown in Figure 3b.

This method differs from usual profiling with Schlumberger arrangement by the use of a third current electrode, (C), placed at "infinity" (OC>4AB). The voltage between M and N is measured when current is transmitted between A and C, B and C and A and B, and three corresponding values of the apparent resistivity calculated, ρAC, ρBC and ρAB.

In head-on profiling the array is kept unchanged and all four electrodes are moved along the profile, with a constant distance between measured points. The resistivity is plotted as a function of the location of the center of the array. Only two of the three resistivity values are independent. The ρAB is just an average of the two other resistivity values and could just as well be calculated from them.

In the case of homogeneous or horizontally layered earth, all the resistivity values are identical. In the vicinity of vertical or nearly vertical resistivity contrasts, the curves for ρ_{AC} and ρ_{BC} versus location behave in different ways. A theoretical head-on resistivity profile across a low

resistivity dike covered with 25 m thick surface layer is shown in Figure 4. The plot of ρ_{AB} shows a minimum directly above the dike but the curves for ρ_{AC-AB} ($=\rho_{AC}-\rho_{AB}$) and ρ_{BC-AB} ($=\rho_{BC}-\rho_{AB}$) have a different sign on each side of the dike and cross directly above it. At the National Energy Authority in Iceland, head-on profiling data is interpreted by a two-dimensional modelling using a finite element program, named: FELIX.

4. RESISTIVITY INTERPRETATION

4.1 One-dimensional Interpretation

4.1.1 Introduction

The resistivity structure below a measuring site can be derived from the measured apparent resistivity curve. In one-dimensional interpretation the basic assumption is that the earth is divided into horizontal layers of infinite extent. The layers are electrically homogeneous and isotropic. A change in resistivity is assured to occur only in one direction i.e. with depth.

In Iceland one-dimensional interpretation is often used for low-temperature areas. Sometimes the conditions are more complicated and the resistivity distribution is clearly two-dimensional or even three-dimensional. In high-temperature areas there are often sharp vertical boundaries around low resistivity areas. Apparent resistivity may appear too low or too high if the current electrodes cross a vertical resistivity boundary.

4.1.2 The inversion program SLINV

SLINV is a non-linear least-square program for inversion of Schlumberger soundings. The program uses an iterative Levenberg-Marquardt inversion algorithm described by H.K.Johansen (1977) together with a forward routine based on the linear filter method as described by H.K.Johansen (1975).

This program was written by Knútur Árnason for the United Nations University Geothermal Training Programme in Reykjavík, Iceland (Knútur Árnason and Gylfi Páll Hersir 1988).

The inversion program SLINV, like most inversion programs,

works in such a way that it reads the measured data points (apparent resistivity curve) and prompts for a starting model. The interpreter guesses, by visual inspection of the data curve, the number of layers and initial model parameters (resistivity values and thicknesses of the layers). The program then iteratively adjusts the resistivity values and layer thicknesses to get the best fit between the measured curve and the curve calculated from the model. It is important to realize that the program does not change the number of layers during the iteration process. It is therefore in most cases necessary to check models with different number of layers to find the model that best fits the data. It is advisable to keep the models simple and the number of layers as few as possible. It should also be kept in mind that the model resulting from inversion can depend on the initial guess and a bad initial guess can lead the inversion process astray. One feature of the program is that a layer parameter, i.e. resistivity and/or thickness of any layer in a model can be fixed during the iteration process. The fixed parameter values determined manually may come from some geological concepts or simply the values may already be known from other studies.

4.1.3 Problems and limitation in one-dimensional interpretation

4.1.3.1 Introduction

Every calculated apparent resistivity value contains a certain error. There are always some errors in reading the transmitted current and the corresponding potential difference. There is also some error in deciding the exact distance between the electrodes. Various things in the surroundings can make shortcuts for the current such as underground cables or pipelines, telephone cables, fences and metallic junk laying on the ground.

If the sounding is placed too close to the sea, the sea-water

can cause shortcut for the current. In the case of a shortcut, the measured potential difference is below the correct value and the measured apparent resistivity value will be too low. Other causes for errors are e.g. due to irregular landscape (hills, valleys).

Resistivity surveying is an efficient way of delineating shallow layered sequences or vertical resistivity discontinuities. It does, however suffer from a number of limitations as outlined by Kearey and Brooks (1984).

- Interpretations are ambiguous. Consequently independent geophysical and geological controls are necessary to discriminate between valid alternative interpretations of the resistivity data. The so-called equivalence layers are an example of this and will be discussed in chapter 4.1.3.3.

- Interpretation is limited to simple structural configurations. Any deviations from these simple situations may be impossible to interpret.

- Topography and the effects of near-surface resistivity variations can mask the effects of deeper variations. Topographic effects are discussed in chapter 4.1.3.2.

- The depth of penetration of the method is limited by the maximum electrical power that can be introduced into the ground and by the practical difficulties of laying out long lengths of cable. The practical depth limit for surveys is about 1 km.

4.1.3.2 Topographic effects

Since geothermal exploration is often done in mountainous terrain where the topography can produce spurious resistivity anomalies, knowledge of the nature of these effects and their inclusion in the interpretation models are important. Treatment of the raw resistivity data obtained from these

rugged areas could produce topographic-related anomalies that may lead to ambiguities in the interpreted models if one does not take into account the significance of topographic effects. Topographic effects are geometric effects which are inherent to the relative locations of the current and potential electrodes and the nature of the terrain itself where resistivity survey lines are carried out. Because of these conditions, current flow lines are distorted with corresponding effect on equi-potential lines. Thus the actual voltage readings get distorted which can be critical to field measurements and data interpretation. Finally it should be mentioned that the topography is a part of the input in the two-dimensional finite element program used at **Orkustofnun** (see chapter 4.2).

4.1.3.3 Equivalence layers

If the earth is horizontally layered, each layer having constant resistivity and if each apparent resistivity value is without error, there is a one-to-one correspondence between resistivity structure and apparent resistivity curve and hence only one solution to our problem. The fit between the measured apparent resistivity curve and the calculated curve from the interpretation model would be perfect. This is never the case though, so the final model will only be obtained within certain limits. There is an ambiguity in the interpretation.

There exist two types of the so-called equivalence layers. Equivalence layers of the s-type occur when a relatively thin layer of low resistivity exists between layers of considerably higher resistivities. For such a layer, it is only the longitudinal conductance (the radio of the thickness and the resistivity) that can be determined with some accuracy. Another type of equivalence layers, called t-type equivalence layers, is also common in one-dimensional resistivity models. They occur when a relatively thin layer with high resistivity is over- and underlain by considerably

lower resistivities. For these layers it is only the transverse resistance (the product of the thickness and the resistivity) that is determined with some accuracy.

4.2 Two-dimensional Interpretation

In two-dimensional interpretation the assumption is made that the resistivity changes with depth and in the direction of the profile but not perpendicular to it.

In two-dimensional interpretation a model is designed of resistivity blocks along a profile, the blocks having different resistivities but infinite extent perpendicular to the profile. The computer then finds apparent resistivity curves corresponding to this model. They are compared to the measured curves. If they do not fit, the model is changed and new curves calculated and recompared and so on until a reasonable fit is obtained between measured and calculated data.

The two-dimensional program used at **ORKUSTOFNUN** is named: FELIX. The topography of the profile is a part of the input in the program. The interpretation program has two units. One of them reads in parameters for defining a two-dimensional vertical section through the earth, including topography as well as locations of all soundings measured over the profile and writes this information in files. It also has options for correcting and changing the model and plotting the model on a paper and a graphics terminal. The model consists of arbitrarily shaped quadrilaterals and triangles and the resistivity is defined as a constant within each of them. The second program is a finite element program which calculates the resistivity curves.

5. INSTRUMENTATION

The equipment needed to conduct resistivity measurements consists of a transmitter unit, for introducing the current into the earth and a receiver unit, for measuring the corresponding potential difference. The instruments in use in Iceland are designed and made in the electronic laboratory at **ORKUSTOFNUN** in cooperation with Örtölvutækni (Microprocessor Technology). The following is a description of the Icelandic equipment.

The transmitter is used for transmitting the current into the ground. The transmitter consists of the following components: Power supply, control module, four inverters and measuring module as well as buttons, switches and meters on the front panel. The transmitter runs on 24 volts DC. It transmits a square wave of variable frequency. The output transmitting power is 500 W.

The receiver consist of a microprocessor module, hand held terminal and three differential input amplifiers. The advantage of having three independent amplifiers is higher efficiency in the measurements of Schlumberger soundings. The microprocessor module is specially designed for this kind of resistivity measurements. It controls the amplifiers and calculates the results of series of measurements. The results of the measurements appear on the terminal as soon as they reach the microprocessor module i.e. the value for transmitting current, the measured potential (between the potential electrodes), the number of measurements made, their mean value and the standard deviation. Each value of the potential obtained is thus the mean value of several measurements. In difficult conditions a few such mean values are collected for measuring one point. Finally a weighted mean value is obtained from all the mean values where the weighting is determined by the standard deviation in each case. The microprocessor then uses the final potential value

for determining the resistivity at that point and the results appear on the terminal

The wire used as connector to the current and potential electrodes is a copper wire, 0.5 mm^2 in diameter with a PVC-insolation. The first 126 m of the current transmitting wire as well as the potential wire are screened. This is done to reduce capacitance and inductive coupling where current wires and potential wires lie parallel. The screen of the potential wire is connected to the frame of the receiver and the screen of the current wire is connected to the frame of the transmitter. The unscreened part of the current wire is kept on reels, three 500 meters reels for each half of the current dipole. To prevent leakage the reels are put in a solid plastic bag at the connection and the innermost reel (closest to the potential electrodes) fastened to a stick so that it does not touch the ground.

The current electrodes are approximately 50 cm long steel poles, 2 cm in diameter (shape of a nail). For current dipoles less than 600 m only one pole is used for each current electrode. With increasing dipole length or high contact resistance between the pole and the earth the number of poles is increased.

The potential electrodes are 12 cm long copper sticks submerged in saturated copper-sulfate solution in a holder. The tip of the holder is made of permeable ceramic. The contact between the electrode and the earth occurs as the solution seeps through the tip.

6. INTERPRETATION OF SCHLUMBERGER SOUNDINGS FROM SAN IGNACIO

6.1 Introduction

The San Ignacio geothermal field is located in the central part of Honduras, approximately 65 km Northeast of the capital, Tegucigalpa. It is at an elevation of 700 m, under the slopes of a mountain-range which reaches 1200 m and borders the wide Siria valley, which has a N60W direction (see Figure 5).

The San Ignacio geothermal field was first investigated during a UN mission in 1976 (Einarsson, 1976; Cuellar, 1976). A geothermal feasibility study was performed by Geonomics (1977). Geochemical investigation and geological mapping was made in 1979-1980 (Gíslason, 1980) and a reconnaissance study in 1987 by Aldrich et al. (1987). Dal and Geotermica Italiana (1988) made extensive studies in San Ignacio including geological mapping, gravimetric, magnetic and resistivity surveys. The resistivity soundings have been interpreted by the author and the results are discussed in this chapter.

Thermal manifestations in Honduras appear to be related to a large-scale thinning and fracturing of the crust in the region, possibly due to large-scale extension (Aldrich et al., 1987). The hot springs in San Ignacio geothermal field are located along several major faults that serve as conduits for the geothermal water (Aldrich et al., 1987). The measured surface temperature ranges from around 50°C to 100°C. Calculated reservoir base temperature, based on geochemical samples is according to Dal and Geotermica Italiana (1988) approximately 200-210°C, but 200°C according to Robert O. Fournier (personal communication, 1988).

6.2 Geological and Geophysical Setting

Figure 5 shows the main geological units and tectonics as

they have been mapped by Dal and Geotermica Italiana (1988). In the immediate vicinity of the San Ignacio geothermal field, paleozoic metamorphic rocks, silicified Padre Miguel Groups tuffs, and alluvial deposits are exposed. The metasediment rocks outcrop extensively and are related to two different metamorphic facies. The first is of low metamorphic grade and includes phyllites, quarzites and marbles while the second is of higher metamorphic grade, granatiferous schists. The metamorphosed igneous rocks are exposed at the north part of the area and are composed of gneiss mylonitic with lenses and strata of greenschists. Augen schists derivated from granitic rocks are mainly composed of quartz, muscovite, biotite and plagioclase. They are found in the zone of thermal manifestations, covering a surface of approximately 15 km^2.

The limestones of Yojoa Group outcrop in the northern east zone, to the south and east of the town Cedros. They are thick to thinly bedded and include also thin intercalations of dolomite and levels of calcareous lutites.

The ignimbrites of Padre Miguel Group are of primarily rhyolitic, rhyodacitic and dacitic composition. The sequence of ignimbritic beds range from well welded to moderately consolidated.

The tectonics of San Ignacio is shown on the geological map in Figure 5. The Siria valley constitutes an asymmetrical graben. The most significant fault system is a system of WNW-trending normal faults that define the northern border of the valley. The elevation of the northern border is greater than the southern one which is affected by a system of normal faults with a small vertical displacement. Another system of faults and fractures is having a traverse direction with respect to the depression. The Arenal-fault, which has a NE-trend is of particular interest since it seems to control the thermal manifestations that are confined to La Tembladera (Aldrich et al., 1987). The Arenal-fault probably also

controlled the upwelling of the El Pedernal dome of rhyolitic composition, southwest of La Tembladera (see Figure 5). The group of faults and fractures that are parallel to the Arenal-fault and restricted to the area around La Tembladera are probably the youngest tectonically activity in San Ignacio. Certainly other faults have controlled the location of springs in the past. Many of the hills along the north side of Siria valley are mantled by older sinter deposits generally at higher elevations than those near the active springs. The older deposits are more extensive, suggesting a long history of thermal activity (Aldrich et al., 1987).

Dal and Geotermica Italiana (1988) have carried out geophysical surveys in San Ignacio during the last two years. The purpose was to identify zones of fracture permeability along the faults and beneath the thin cover of valley fill of conglomerates and sandstones. A part of this project was the drilling of a 500 m deep borehole, 1-1.5 km south of La Tembladera. The location of the borehole is shown on Figure 5 and the temperature logs are given in Figure 6.

The gravimetric and magnetic surveys showed the followings results (Dal and Geotermica Italiana, 1988):

- The main structural trend has a direction N70W-N80W. In the northern part of the area this corresponds to series of subvertical faults that constitute a structure similar to a graben.

- A geological body characterized by high density and magnetic susceptibility is located in the western part of Siria valley, south of El Porvenir and El Terrero. It is about 5 km long and lies between The Quebrachal zone and an airstrip. The edges of this body are in general very sloped and it might constitute a basic intrusive body.

- The area of surface manifestations around La Tembladera is located approximately along a zone characterized by a

magnetic high. This indicates that the upwelling of the thermal water is along a fracture-plane, where there is no lateral infiltration and insignificant hydrothermal alteration.

The manifestations are associated with a small gravimetric minimum, elongated in the SW-NE direction.

6.3 Resistivity Soundings

6.3.1 Introduction

A total of 85 Schlumberger soundings were performed between January and May 1987 by Dal and Geotermica Italiana (1988). The location of the soundings is shown on Figure 7. They are orientated either perpendicular or parallel to the graben.

In this report the results of a one-dimensional interpretation of 81 Schlumberger soundings is shown together with the results of a two-dimensional interpretation of one profile. The aim of the interpretation was to look for a low resistivity anomaly and to get a general picture of the resistivity structure of the area.

6.3.2 One-dimensional interpretation

A non-linear least-square inversion program described in chapter 4.1.2 was used to interpret the Schlumberger soundings from the San Ignacio area. The program assumes that the earth is horizontally stratified with each layer electrically homogeneous and isotropic. It calculates the apparent resistivity curve from a given model, compares it with the measured curve, adjusts the model, calculates a new curve, recompares and so on until a reasonable fit between measured and calculated data is reached. The results of the one-dimensional interpretation for each sounding and the corresponding calculated and measured apparent resistivity curves are shown in appendix I.

Seven resistivity cross-sections have been made. Their locations are shown in Figure 7. Five cross-sections lay across the Siria valley (Figures 8-12) and two along the valley (Figures 13 and 14). Three iso-resistivity maps were made as well, showing resistivity at 500 m, 400 m and 300 m above sea-level (Figures 15-17).

Here each resistivity cross-section and iso-resistivity map will be described.

Resistivity cross-section A-A′ (Figure 8), crosses the eastern part of Siria valley. It includes 6 soundings with half the current electrode spacing (AB/2) generally extending upto 700-1500 m. The surface layers are thin and have a resistivity of more than 100 Ωm. They correspond to a thin cover of valley fill, foothill deposits and alluvial deposits which cover most of the surface in the area. Beneath the surface layers, in the southwest part of the section, there is a low-resistivity layer of 5 to 10 Ωm, about 100 m thick. This low-resistivity layer might be correlated to old alluvial deposits or clay. Beneath the surface layers in the rest of the section there is a layer of 10 to 50 Ωm resistivity. It is 100-500 m thick and might be correlated to a sandstones and conglomerates (Red beds). Beneath these layers there is a high resistivity layer, of more than 50 Ωm. It reflects, most likely, the metamorphic basement. This layer will hereafter be called the resistive-basement.

Resistivity cross-section B-B′ (Figure 9), includes 7 soundings with half the current electrode spacing ranging upto 1000-2000 m. As in profile A-A′ the surface layers can be correlated to a thin cover of valley fill. Beneath the surface layers there is low-resistivity layer (5-10 Ωm) with an average thickness of 100 m. This layer is thicker in the southernmost part of the section. Beneath this layer there is another low-resistivity layer of less than 5 Ωm and about 100-200 m thick. It may either represent clay deposits or a structure of the area connected with the geothermal system.

Clay deposits is a more likely explanation. These low-resistivity layers are not present beneath the northernmost sounding (n200).

Resistivity cross-section C-C' (Figure 10), crosses the central part of the valley. It includes 7 soundings with half the current electrode spacing ranging upto 1500-3000 m. In this cross-section only three resistivity layers were identified. The surface layer, a low-resistivity layer (5-10 Ωm) and the resistive-basement. The low-resistivity layer is present in all the soundings and has a thickness of about 300 m Five soundings from this profile have been interpreted two-dimensionally. The results are discussed in section 6.3.3.

Resistivity cross-section D-D' (Figure 11), crosses the western part of the valley. It includes 9 soundings. In this section the low-resistivity layer (5-10 Ωm) is only some 50 m thick and restricted to the northern part of the section (middle of the valley). The resistive-basement is at rather shallow depth.

Resistivity cross-section E-E' (Figure 12), is the westernmost section which runs through the valley. Low resistivity layer (5-10 Ωm) is only present in the two northernmost soundings (n236 and n237), southwest of El Porvenir. The resistive-basement is at very shallow depth in this section, 500 m a.s.l. except for the southernmost sounding (n213), where it is at 300 m a.s.l.

Resistivity cross-section F-F' (Figure 13), runs along the middle of the valley. It includes 13 soundings with half the current electrode spacing generally extending upto 700-3000 m. The resistivity layering is similar to the other profiles described above. Low-resistivity layer is found in all the section except beneath the western- and easternmost soundings. The thickness varies from 50 to 250 m. The resistivity of this layer is especially low (< 5 Ωm) on the

part of the section which lays south of El Terrero and La Tembladera.

Resistivity cross-section G-G' (Figure 14), runs along the northern side of the valley and is almost parallel to section F-F'. It includes 12 soundings with half the current electrode spacing generally extending upto 700-2000 m. The geological stratigraphy of the borehole has been projected into the section (Dal and Geotermica Italiana, 1988). The borehole is located, where abrupt horizontal resistivity changes occur. It is therefore almost impossible to correlate the lithology in the borehole to the resistivity layering. It seems though reasonable to conclude that the surface resistivity layers reflect the alluvial deposits, seen in the borehole. Low-resistivity is found south of El Terrero and in particular southwest of La Tembladera.

Iso-resistivity maps: The general picture of the resistivity structure at the San Ignacio geothermal field is shown on three iso-resistivity maps. Figure 15 show the resistivity at 500 m above sea-level, Figure 16 shows the resistivity at 400 m above sea-level and Figure 17 shows the resistivity at 300 m above sea-level. The maps are based on the one-dimensional interpretation of the Schlumberger resistivity soundings. The model for each sounding is shown in appendix I. Most of the models appear in the resistivity cross-sections which have already been described in this chapter. The resistivity values at the appropriate depths are written on the maps in Ωm for each sounding and iso-resistivity lines have been drawn. At 500 m a.s.l. (Figure 15) there is a low resistivity anomaly (resistivity less than 10 Ωm) in Siria valley running from La Tembladera in the east. The anomaly is rather wide between La Tembladera and El Terrero. There it becomes a narrow strip stretching to the west as far as Schlumberger soundings have been made. At 400 m a.s.l. (Figure 16) the anomaly is restricted to the area southwest of La Tembladera. At 300 m a.s.l. (Figure 17) the anomaly is even smaller and the resistive-basement (resistivity higher

than 50 Ωm) covers most of the map. The part of the low-resistivity anomaly which is present at 500 m a.s.l. but absent at 400 m a.s.l. is most likely caused by alluvial deposits. Comparison with the geological map (Figure 5) shows the correlations between the alluvial deposits and the low-resistivity anomaly at 500 m a.s.l. On the other hand the low-resistivity anomaly southwest of La Tembladera, the area where geothermal surface manifestations are confined, is probably related to the geothermal field. The geological and geothermal interpretation of the resistivity structure is the task of chapter 6.4.

6.3.3 Two-dimensional interpretation

One-dimensional interpretation of Schlumberger soundings can often be misleading if the earth if far from being horizontally layered. In two-dimensional interpretation the resistivity is assumed to change both with depth and in the direction of the profile but not perpendicular to it. Two-dimensional interpretation is described in chapter 4.2.

One profile from the San Ignacio geothermal field has been interpreted two-dimensionally, profile C-C'. Its location and the associated 5 Schlumberger soundings are shown in Figure 6. Only soundings laying parallel to the profile can be used. The resistivity cross-section resulting from the one-dimensional interpretation (Figure 10) was used as a starting model for the two-dimensional interpretation. After the model had been changed 10 times, an acceptable model was found. It is shown in Figure 18. The location of the Schlumberger soundings on the profile is shown as well. The curves for the calculated and measured apparent resistivity is shown in appendix II. They show that the model data fits pretty well with the measured data for each sounding.

The two-dimensional model is similar to the one-dimensional model but it seems to be more trueworthy. It shows surface layer/layers, a low-resistivity layer of different

resistivity (4-10 Ωm) and beneath it is what has been called the resistivity-basement (100 and 200 Ωm). The low-resistivity anomaly is only (4-5 Ωm) between soundings n206 and n208. This is in the middle of the low-resistivity anomaly at 400 m a.s.l. The two-dimensional interpretation shows that the resistivity of this anomaly is twice as high to the north of sounding n208.

Since the model from the two-dimensional interpretation is similar to the model from the one-dimensional interpretation it leads one to conclude that the area, at least around this part of the valley, is electrically rather one-dimensional.

6.4 Results

The results of the interpretation of the Schlumberger soundings can be summarized in the following. Almost all the soundings were located in the Siria valley which is filled with alluvial deposits. The interpretation of the resistivity soundings revealed that the deposits have relatively low resistivity and hence obscured possible interesting resistivity structure in the underlying basement.

Comparison with modelling of the Bouguer gravity data (Dal and Geotermica Italiana, 1988) shows that estimation of the thickness of the valley filling is in good agreement with the depth to the resistive-basement as revealed by the resistivity interpretation. At 400 m a.s.l. the iso-resistivity map (Figure 16) shows a low-resistivity anomaly (less than 6 Ωm) southwest of La Tembladera covering an area of about 15 km^2. All the geothermal surface manifestations (see Figure 5) lay outside and to the north of this area. At first glance there is no obvious connection between this low-resistivity anomaly and geothermal fluids. The surface manifestations north of the anomaly are at higher elevation than the bottom of the valley and it is therefore rather unprovable that they are fed by an upflow located in the resistivity anomaly. On the other hand the surface

manifestations are found where the zone of most recent tectonic activity, west of the Arenal-fault, intersects one of the faults bordering the northern part of the Siria valley. This together with the presence of the sinter deposits north of La Tembladera might suggest that the geothermal activity is connected to the youngest tectonic faults with the NE-SW trend.

The low-resistivity anomaly discussed above is in the southwest extension of the most recent tectonics and could be caused by geothermal fluids conducted by these faults and infiltrated into the valley filling. This may seem to be in contradiction to the conclusion drawn from the results of the drilling of the borehole but it is located at the easter border of the low-resistivity anomaly and hence outside the region of infiltration. If this is the case then it is not to be expected to see an extensive low-resistivity anomaly in the basement because the geothermal fluids are confined to the fractures and will not produce wide spread anomalies at the shallow depths observable by the resistivity soundings. It is therefore probable that a detailed resistivity survey of the area surrounding the surface manifestations and in particular the area north of them is needed to locate flow paths and feasible drilling targets. The first phase in such a survey could be to make Schlumberger soundings, densely spaced (of no more than 500 m between soundings) and oriented along the profiles, both parallel and perpendicular to the valley. It is to be expected that a two-dimensional modelling of the data will be necessary. Resistivity head-on profiling along the profiles can be added later, if necessary in order to delineate nearly vertical aquifers.

7. DISCUSSION

There are many methods of resistivity surveying. Some make use of the naturally occurring electromagnetic field within the earth while others require the introduction of artificially generated current into the ground. In this report two resistivity methods are described, Schlumberger soundings and head-on profiling.

The one-dimensional interpretation of resistivity soundings was made in the early days with the help of master curves of the apparent resistivity. At the present iterative methods which make use of the linear filter method are extensively in use. In this report one-dimensional interpretation using a non-linear least-square program for inversion of Schlumberger soundings was used to interpret resistivity data. A short description of the program is outlined in the report. Two-dimensional interpretation of resistivity data is also mentioned.

81 Schlumberger soundings which were performed in the San Ignacio geothermal field in Honduras have been interpreted. The results of this interpretation are described in the report. They have proven to be of importance in the understanding of the geothermal field. It would have been better though if more soundings were made, more densely and covering a bigger area. As always an integrated interpretation of geological and all available geophysical results was necessary to bring out the geothermal meaning of the results.

8. CONCLUSION

1. Schlumberger resistivity soundings from San Ignacio geothermal field in Honduras have been interpreted one-dimensionally. Most of them were confined to the Siria valley which is filled with alluvial deposits. The results revealed that the deposits have a relatively low resistivity and hence obscured possible interesting resistivity structure in the underlaying basement. No soundings were made around the hot springs in La Tembladera, except south of the area.

2. Comparison between the interpretation of gravity data and resistivity data shows that the estimation of the thickness of the valley filling is in good agreement with the depth to the resistive-basement.

3. Surface manifestations are located, where a NE-trending zone of most recent tectonic activity, west of the Arenal-fault, intersects a WNW-trending fault bordering the northern part of the Siria valley. A low-resistivity anomaly is present at 400 m a.s.l. in the southwest extension of this zone, covering an area of 15 km^2. All this together with the presence of sinter deposits north of La Tembladera might suggest that the geothermal activity is related to this NE-trending fault zone and the low-resistivity could be caused by geothermal fluids conducted by these faults and infiltrated into the valley filling. The only borehole in San Ignacio is on the easternmost edge of this area.

4. A more detailed resistivity survey of the area around the hot springs in La Tembladera and a better understanding of the geology of the area, alteration and tectonics, is suggested in order to find the flow paths and feasible drilling targets.

ACKNOWLEDGEMENTS

I express my profound gratitude to my advisor, Gylfi Páll Hersir geophysicists at the National Energy Authority, for his support of this project, his fertile discussions and his patient guidance during the training course and the preparation of this report.

Many thanks to Knútur Árnason and Ólafur Flóvenz who both critically reviewed the manuscript.

Thanks are also due to the staff of the UNU Geothermal Training Programme, especially to its director Jón-Steinar Gudmundsson for his valuable assistance.

Finally my thanks also go to Auður Ágústsdóttir for having helped me with my drawings.

REFERENCES

Archie, G.E. (1942) : "The electrical Resistivity Log As An Aid In Determining Some Reservoir Characteristics," Trans AIME, 146, 54-67.

Aldrich, M.J. et al. (1987) : "San Ignacio (La Tembladera) Geothermal Site, Departamento de Francisco Morazán, Honduras,

Central America. Geological Field Report," Los Alamos National Laboratory, New Mexico 87545.

Árnason, K., and Hersir, G.P. (1988) : "One-dimensional Inversion Schlumberger Resistivity Soundings. Computer Program, Description and User's Guide," UNU report 1988 - 8

Árnason, K., and Hersir, G.P. (1988) : "Geophysical Survey at Nesjavellir High-Temperature Area, SW-Iceland," Manuscript.

Cheng, Y.W. (1980) : "Location of Near Surface Faults in Geothermal Prospects by the Combined Head-on Resistivity Profiling Method," Proceedings of the New Zealand Geothermal Workshop 1980, 163-166.

Cuellar, C. (1976) : "Característica Químicas, Areas Geotermicas de Honduras," (Informe Preliminar). Unpublished report.

Dal in.te.sa. SpA., and Geotermica Italiana srl. (1988) : "Estudio de Pre-Factibilidad Geotermica en la Region Central de Honduras," Proyecto: HON/85/001.

Dakhnov, V.N. (1962) : "Geophysical Well Logging," Q. Colo. Sch. Mines, 57 (2), 445 pp.

Duba, A., A.J. Piwinskii, M. Santor, and H.C. Weed. (1978) : "The Electrical Conductivity of Sandstone, Limestone and Granite," Geophys. J.R. Astron. Soc., 53, 583-597.

Einarsson, S.S. (1976) : "Report on Prelimary Reconnaissance of Geothermal Manifestations in Honduras," Draft report for UNDP Project HON/14/004.

Flóvenz, Ó.G,. and Georgsson, L.S. (1982) : "Prospecting for Near Vertical Aquifers in Low Temperature Geothermal Areas in Iceland," G.R.C. Transactions, V. 6, (in press).

Flóvenz, Ó.G. (1984) : "Application of the Head-on Resistivity Profiling Method in Geothermal Exploration," Geothermal Resources Council Transactions. Vol. 8, 493-498.

Flóvenz, Ó.G., Georgsson, L.S., and Árnason, K. (1985) : "Resistivity Structure of the Upper Crust in Iceland," Journal of Geophysical Research. Vol 90, NO. B12, 10.136-10.150.

Geonomics Inc. (1977) : "Report of Geothermal Feasibility Studies in Honduras," Unpublished report prepared for mid-project meeting for ENEE, Honduras, 2 volumes.

Gíslason G. (1980) : "Report of the Activities and Interpretation of Results of the Geothermal Project of Honduras," RLA/76/012, 2 volumes.

Hersir, G.P. (1988) : "Geophysical Lecture Notes," UNU Geothermal Training Programme, Iceland.

Hochstein, M.P. (1982) : "Introduction to Geothermal Prospecting," Geothermal Institute, University of Auckland.

Johansen, H.K. (1975) : "An Interactive Computer/Graphic-Display-Terminal System for Interpretation of Resistivity Soundings," Geophysical Prospecting 23, pp. 449-458.

Johansen, H.K. (1977) : "A Man/Computer Interpretation System for Resistivity Soundings Over a Horizontally Stratified Earth," Geophysical Prospecting 25, pp. 667-691.

Kearey, P., and Brooks, M. (1984) : "An Introduction to Geophysical Exploration," Blackwell Scientific Publications, 296 pp.

Keller, G.V., and Frischknecht, F.C. (1966) : "Electrical Methods in Geophysical Prospecting," Pergamon Press, 517 pp.

Koefoed, O. (1979) : "Geosounding Principles, 1. Resistivity Sounding Measurements," Elsevier Scientific Publishing Company.

Lumb, J.T. (1981) : "Prospecting for Geothermal Resources," pp. 77-108. From: Geothermal Systems: Principles and Cases histories. Editors: Rybach, L., and Muffler, L.J.P., John Wiley & Sons, 359 pp.

Quist, A.S., and Marshall, W.L. (1968) : "Electrical Conductances of Aqueous Sodium Chloride Solutions from 0 to 800°C and at Pressures to 4000 Bars," Journ. Phys. Chem., 72: 684-703.

Risk, G.F., Macdonald, W.J.P., and Dawson, G.B. (1970) : "Resistivity Surveys of the Broadlands Geothermal Region, New Zealand," Geothermics, special issue 2, 2, 287-294.

Ucok, H. (1979) : "Temperature Dependance of the Electrical Resistivity of Aqueous Salt Solutions and Solution-Saturated Porous Rocks," PhD thesis, Dpto of Petrol. Engr., Univ. of So. Calif., 154p.

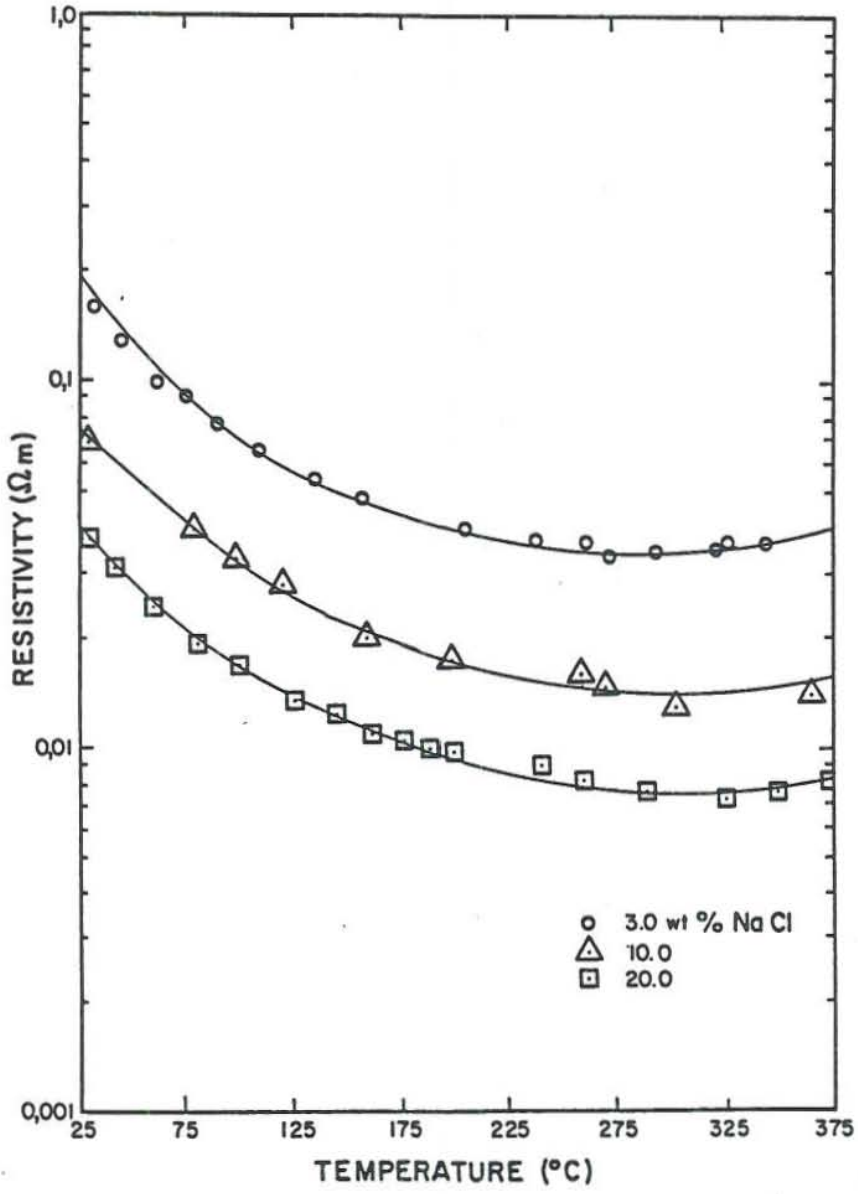

Figure 1. Resistivity versus temperature and salinity. Taken from Ucok (1979)

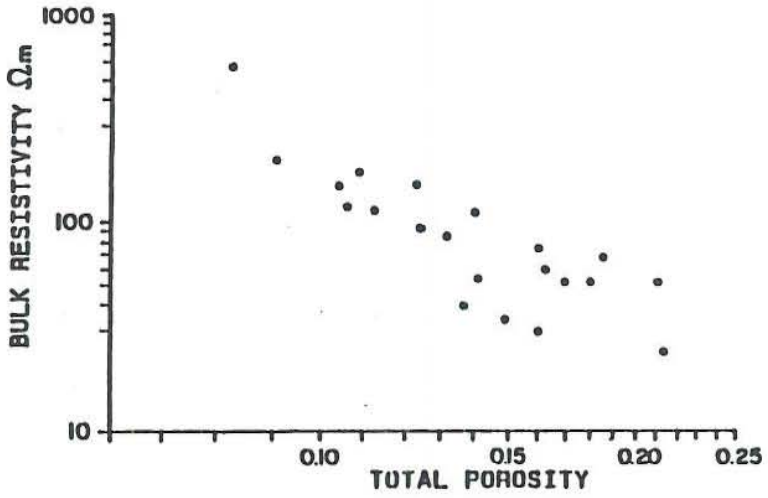

Figure 2. Resistivity versus porosity. Taken from Flóvenz et al. (1985)

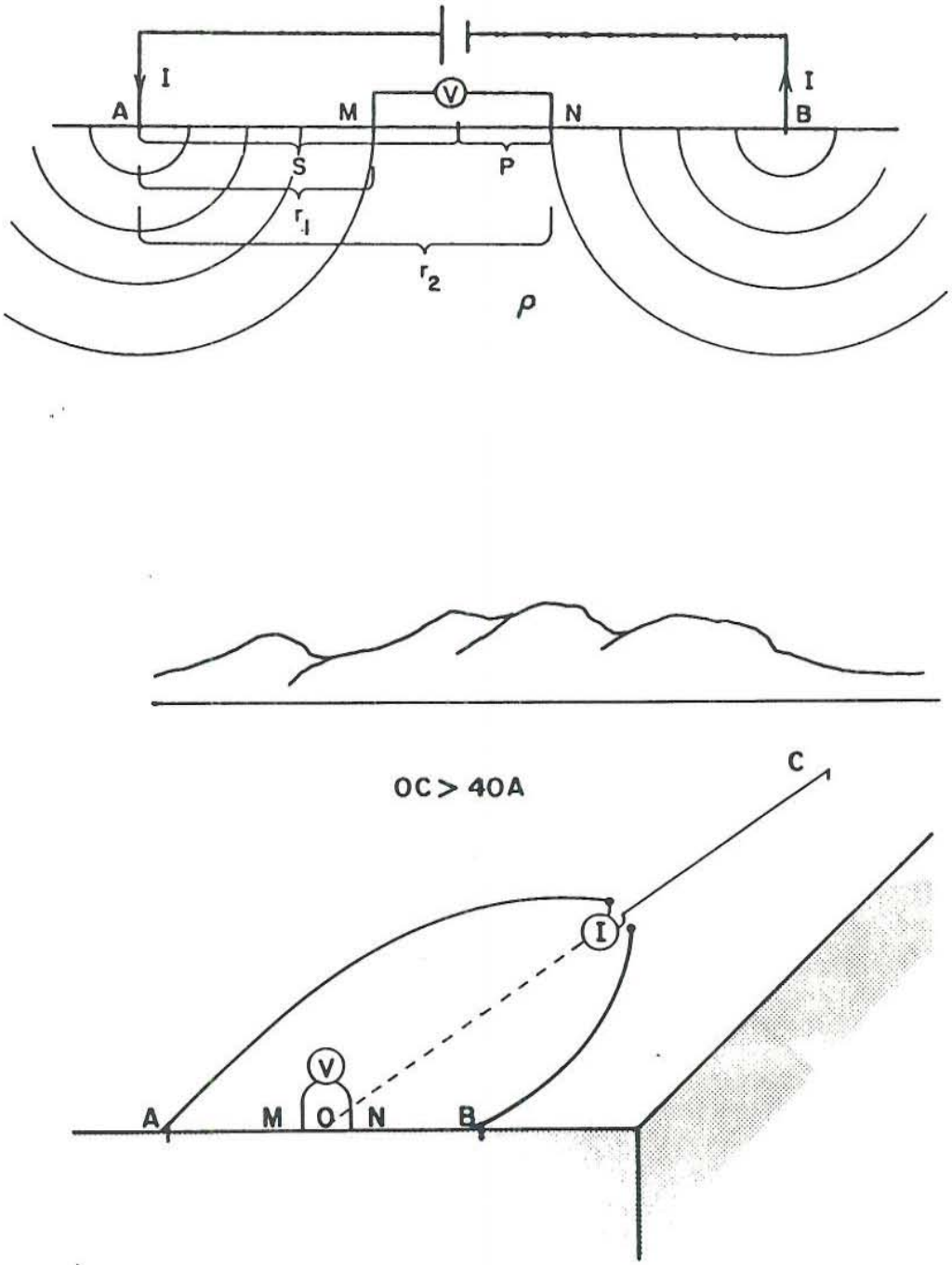

Figure 3. Schlumberger and head-on configurations. The uppermost figure shows the Schlumberger configuration while the lowermost one shows the head-on configuration

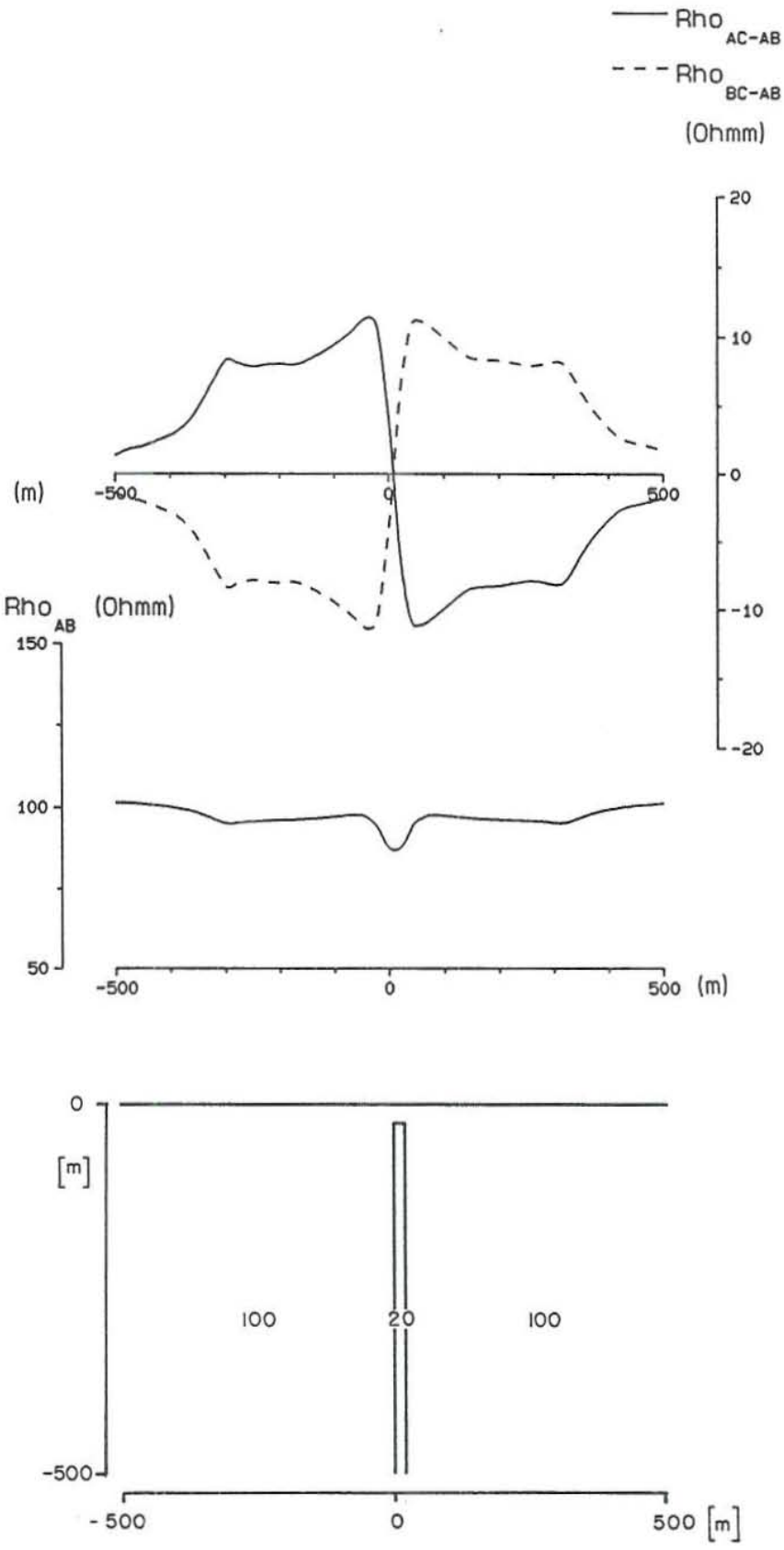

Figure 4. Head-on profiling, an example. The lowermost Figure shows the model and the uppermost one the corresponding apparent resistivity curves (AB/2 = 300 m)

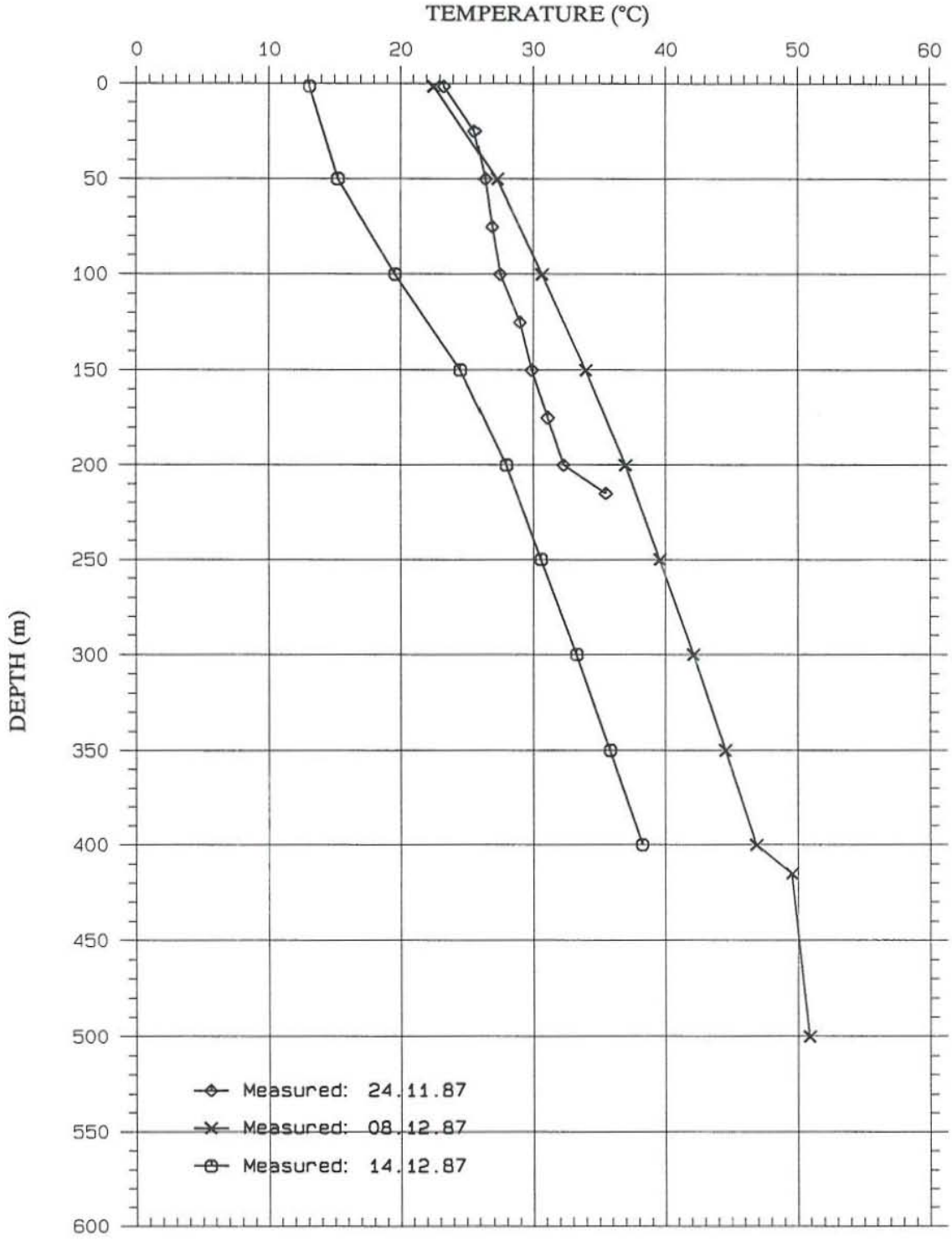

Figure 6. Temperature log from the borehole, for location see Figure 5. Taken from Dal and Geotermica Italiana (1988)

APPENDIX I

One-dimensional interpretation
of Schlumberger soundings:

Models, corresponding calculated apparent resistivity curves (shown as continuous curves) and measured apparent resistivity curves (shown as points)

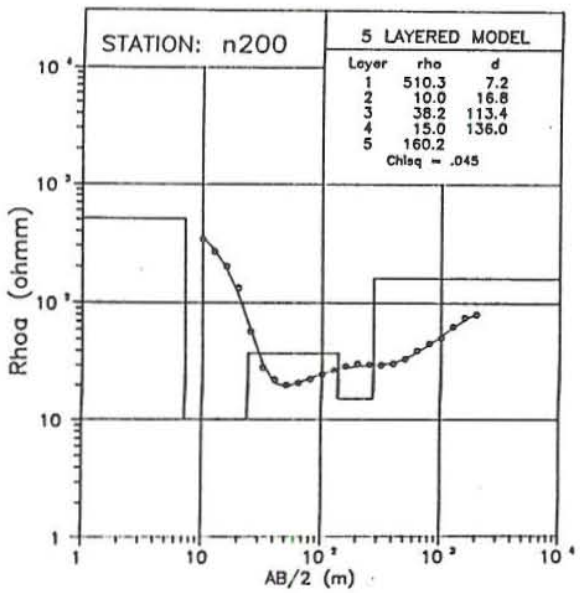
STATION: n200
5 LAYERED MODEL
Layer rho d
1 510.3 7.2
2 10.0 16.8
3 38.2 113.4
4 15.0 136.0
5 160.2
Chisq = .045
Rhoa (ohmm)
AB/2 (m)

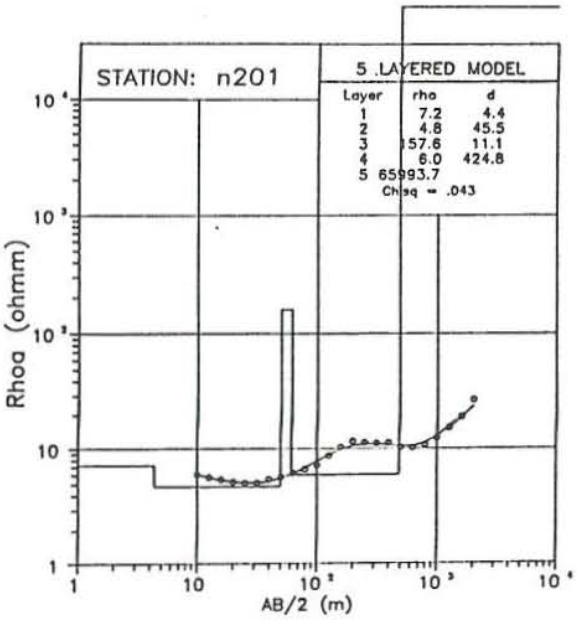
STATION: n201
5 LAYERED MODEL
Layer rho d
1 7.2 4.4
2 4.8 45.5
3 157.6 11.1
4 6.0 424.8
5 65993.7
Chisq = .043
Rhoa (ohmm)
AB/2 (m)

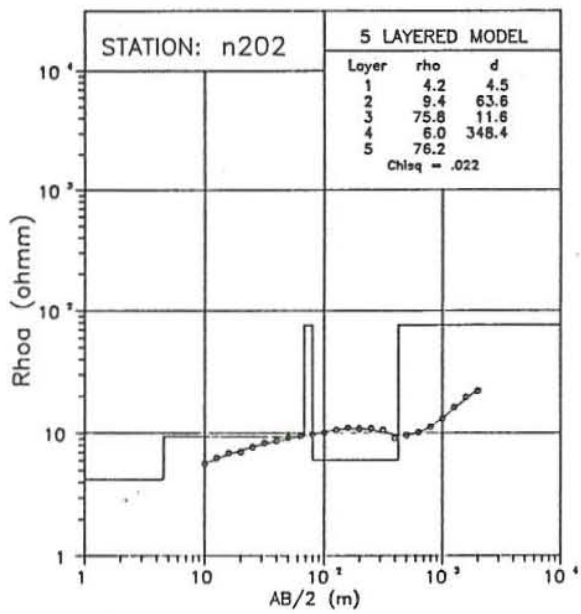
STATION: n202
5 LAYERED MODEL
Layer rho d
1 4.2 4.5
2 9.4 63.6
3 75.8 11.6
4 6.0 348.4
5 76.2
Chisq = .022
Rhoa (ohmm)
AB/2 (m)

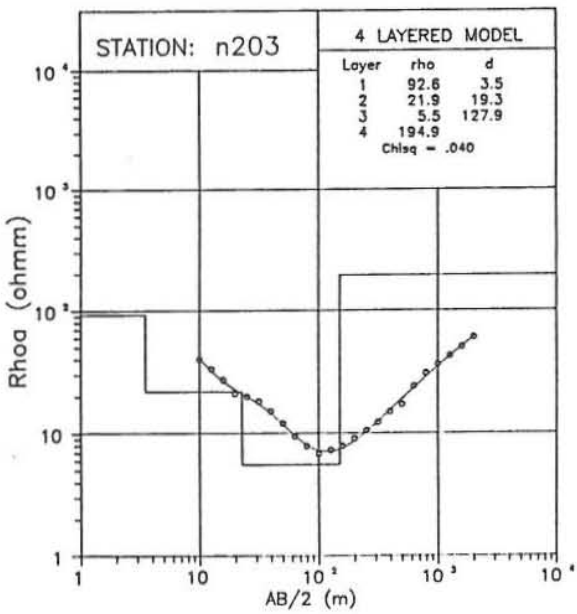
STATION: n203
4 LAYERED MODEL
Layer rho d
1 92.6 3.5
2 21.9 19.3
3 5.5 127.9
4 194.9
Chisq = .040
Rhoa (ohmm)
AB/2 (m)

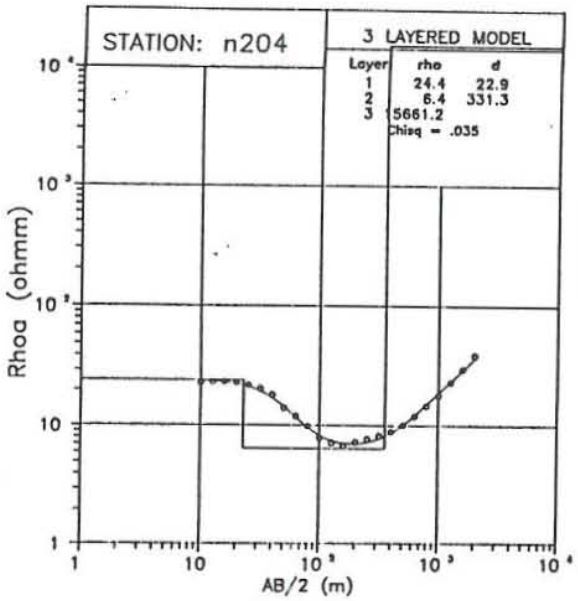
STATION: n204
3 LAYERED MODEL
Layer rho d
1 24.4 22.9
2 6.4 331.3
3 5661.2
Chisq = .035
Rhoa (ohmm)
AB/2 (m)

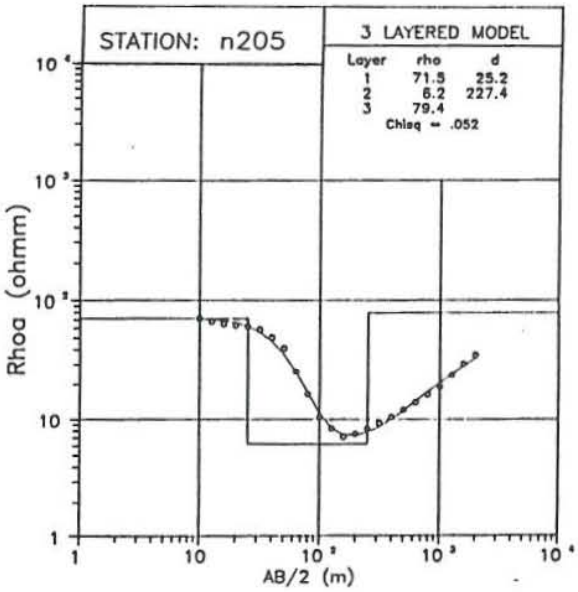
STATION: n205
3 LAYERED MODEL
Layer rho d
1 71.5 25.2
2 6.2 227.4
3 79.4
Chisq = .052
Rhoa (ohmm)
AB/2 (m)

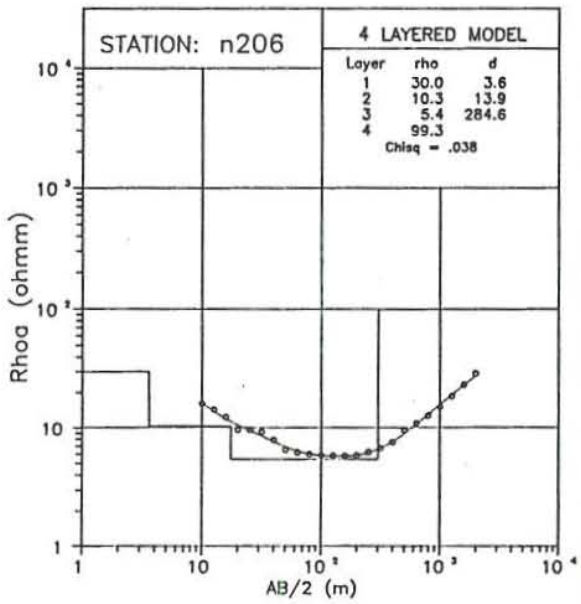
STATION: n206
4 LAYERED MODEL
Layer rho d
1 30.0 3.6
2 10.3 13.9
3 5.4 284.6
4 99.3
Chisq = .038
Rhoa (ohmm)
AB/2 (m)

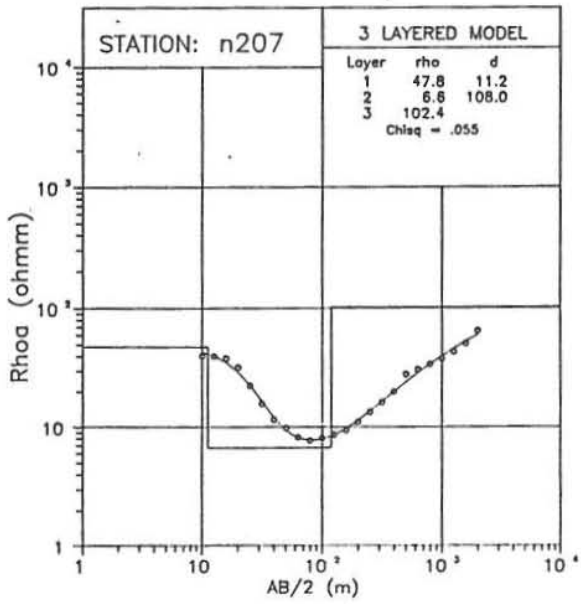
STATION: n207
3 LAYERED MODEL
Layer rho d
1 47.8 11.2
2 6.6 108.0
3 102.4
Chisq = .055
Rhoa (ohmm)
AB/2 (m)

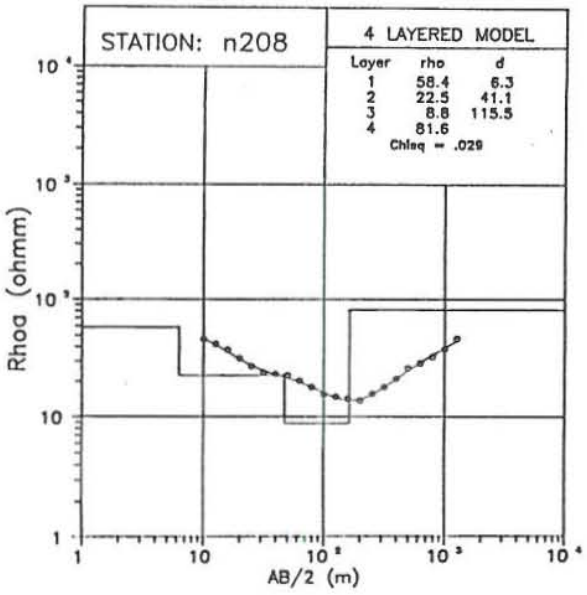
STATION: n208
4 LAYERED MODEL
Layer rho d
1 58.4 6.3
2 22.5 41.1
3 8.8 115.5
4 81.6
Chisq = .029
Rhoa (ohmm)
AB/2 (m)

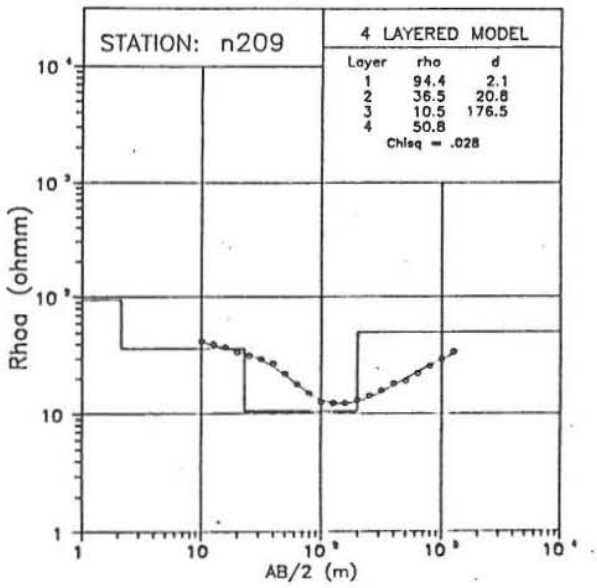
STATION: n209
4 LAYERED MODEL
Layer rho d
1 94.4 2.1
2 36.5 20.8
3 10.5 176.5
4 50.8
Chisq = .028
Rhoa (ohmm)
AB/2 (m)

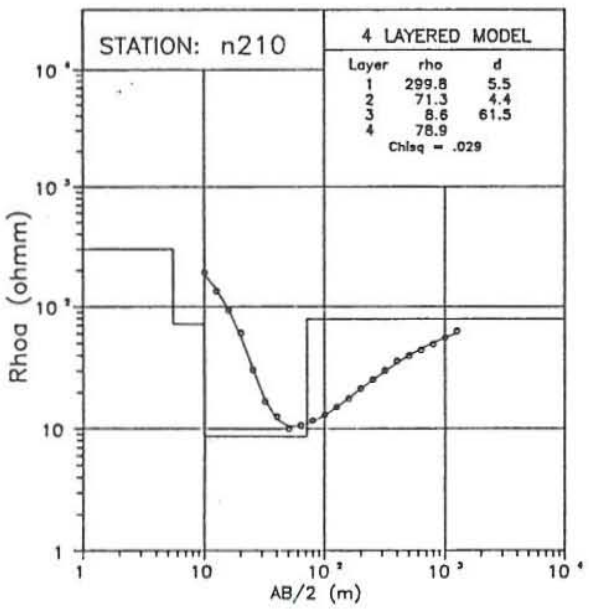
STATION: n210
4 LAYERED MODEL
Layer rho d
1 299.8 5.5
2 71.3 4.4
3 8.6 61.5
4 78.9
Chisq = .029
Rhoa (ohmm)
AB/2 (m)

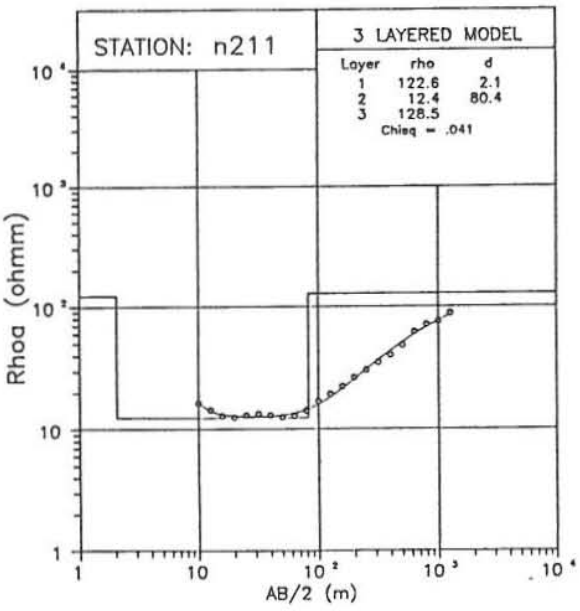
STATION: n211
3 LAYERED MODEL
Layer rho d
1 122.6 2.1
2 12.4 80.4
3 128.5
Chisq = .041
Rhoa (ohmm)
AB/2 (m)

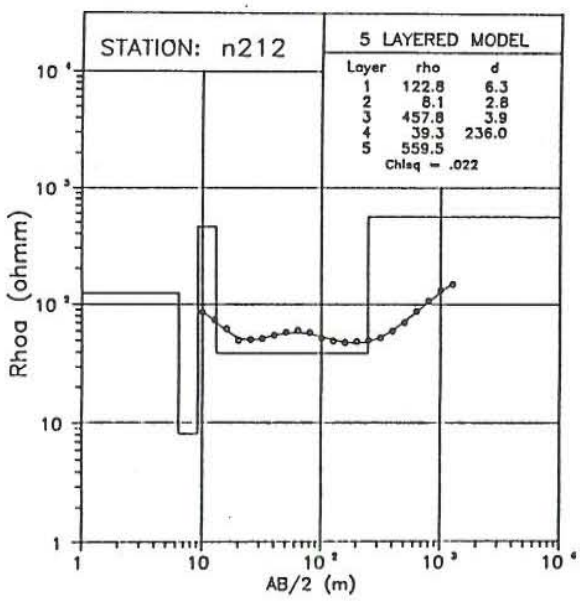
STATION: n212
5 LAYERED MODEL
Layer rho d
1 122.8 6.3
2 8.1 2.8
3 457.8 3.9
4 39.3 236.0
5 559.5
Chisq = .022
Rhoa (ohmm)
AB/2 (m)

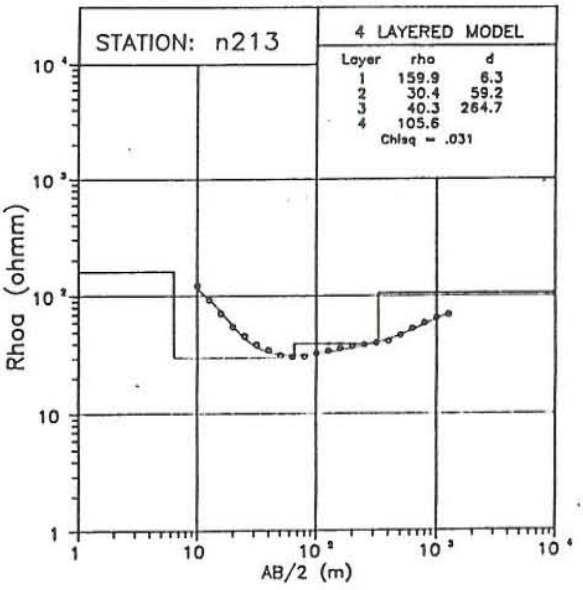
STATION: n213
4 LAYERED MODEL
Layer rho d
1 159.9 6.3
2 30.4 59.2
3 40.3 264.7
4 105.6
Chisq = .031
Rhoa (ohmm)
AB/2 (m)

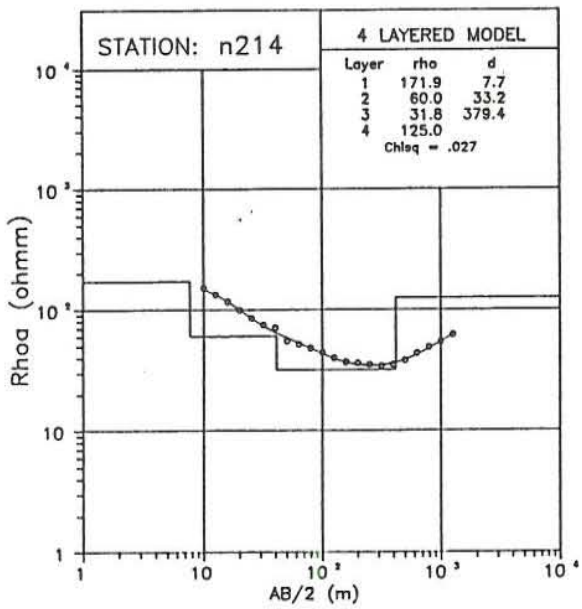
STATION: n214
4 LAYERED MODEL
Layer rho d
1 171.9 7.7
2 60.0 33.2
3 31.8 379.4
4 125.0
Chisq = .027
Rhoa (ohmm)
AB/2 (m)

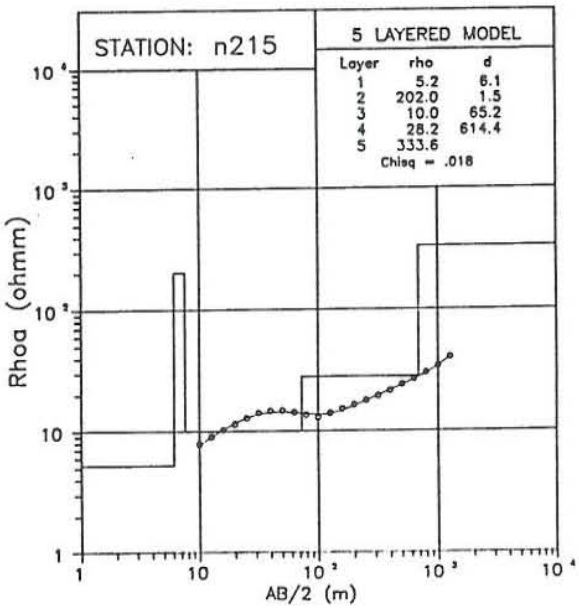
STATION: n215
5 LAYERED MODEL
Layer rho d
1 5.2 6.1
2 202.0 1.5
3 10.0 65.2
4 28.2 614.4
5 333.6
Chisq = .018
Rhoa (ohmm)
AB/2 (m)

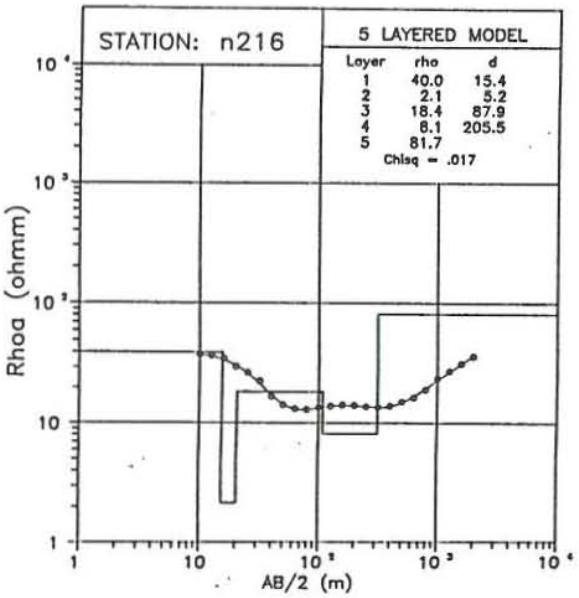
STATION: n216
5 LAYERED MODEL
Layer rho d
1 40.0 15.4
2 2.1 5.2
3 18.4 87.9
4 8.1 205.5
5 81.7
Chisq = .017
Rhoa (ohmm)
AB/2 (m)

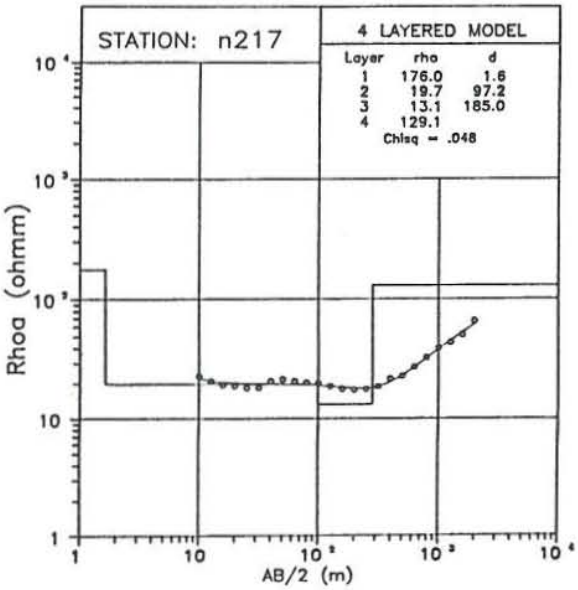
STATION: n217
4 LAYERED MODEL
Layer rho d
1 176.0 1.6
2 19.7 97.2
3 13.1 185.0
4 129.1
Chisq = .048
Rhoa (ohmm)
AB/2 (m)

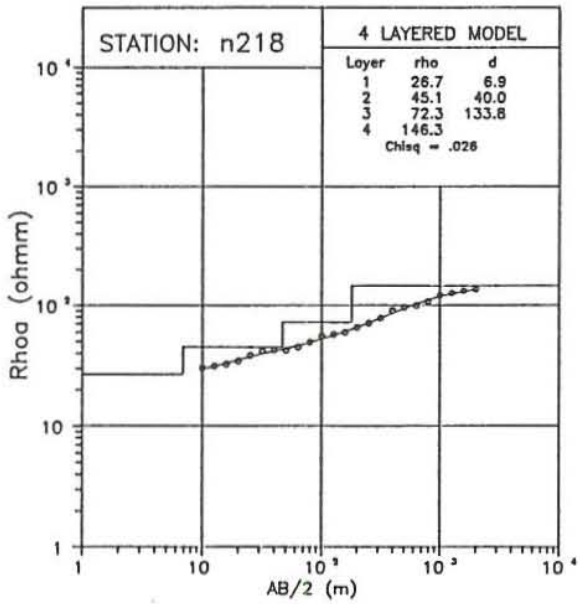
STATION: n218
4 LAYERED MODEL
Layer rho d
1 26.7 6.9
2 45.1 40.0
3 72.3 133.8
4 146.3
Chisq = .026
Rhoa (ohmm)
AB/2 (m)

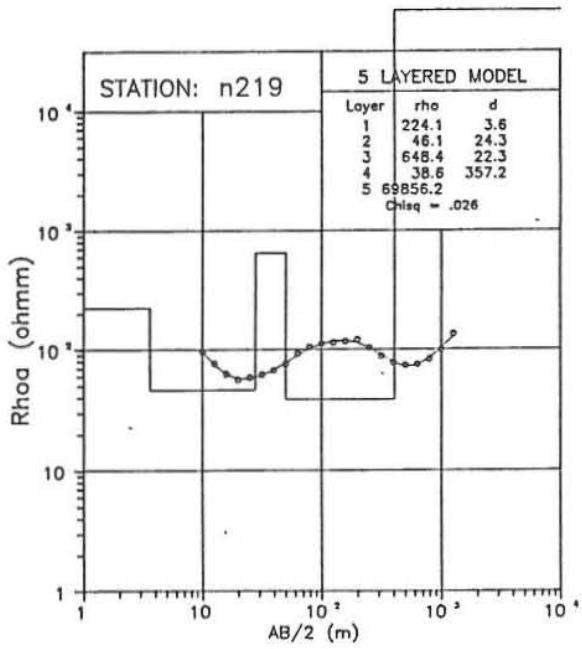
STATION: n219
5 LAYERED MODEL
Layer rho d
1 224.1 3.6
2 46.1 24.3
3 648.4 22.3
4 38.6 357.2
5 69856.2
Chisq = .026
Rhoa (ohmm)
AB/2 (m)

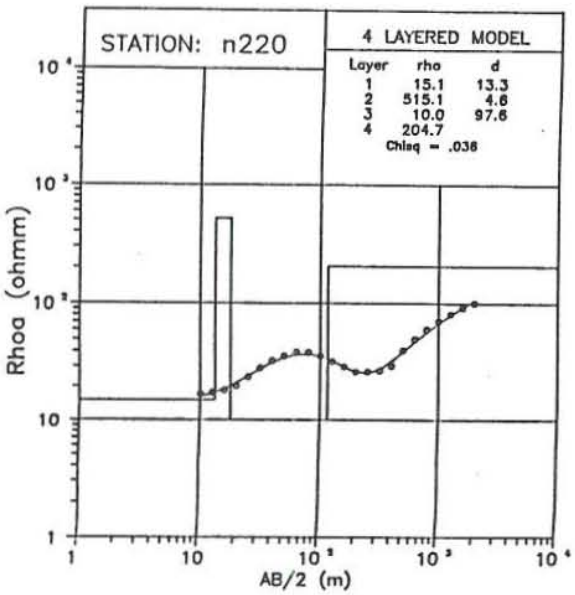
STATION: n220
4 LAYERED MODEL
Layer rho d
1 15.1 13.3
2 515.1 4.6
3 10.0 97.6
4 204.7
Chisq = .036
Rhoa (ohmm)
AB/2 (m)

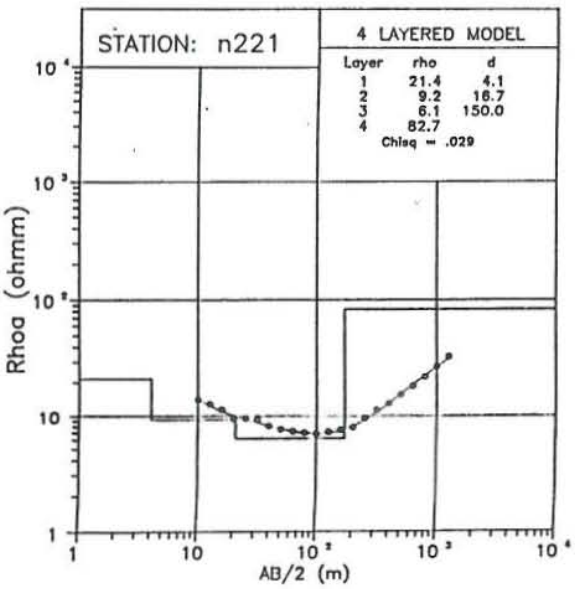
STATION: n221
4 LAYERED MODEL
Layer rho d
1 21.4 4.1
2 9.2 16.7
3 6.1 150.0
4 82.7
Chisq = .029
Rhoa (ohmm)
AB/2 (m)

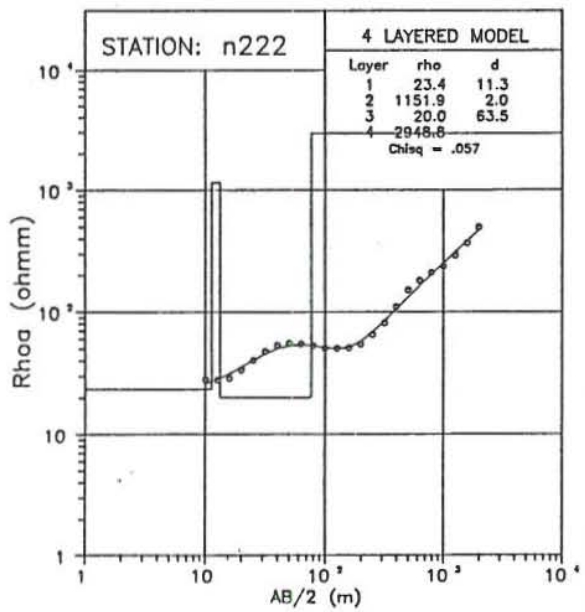
STATION: n222
4 LAYERED MODEL
Layer rho d
1 23.4 11.3
2 1151.9 2.0
3 20.0 63.5
4 2948.8
Chisq = .057
Rhoa (ohmm)
AB/2 (m)

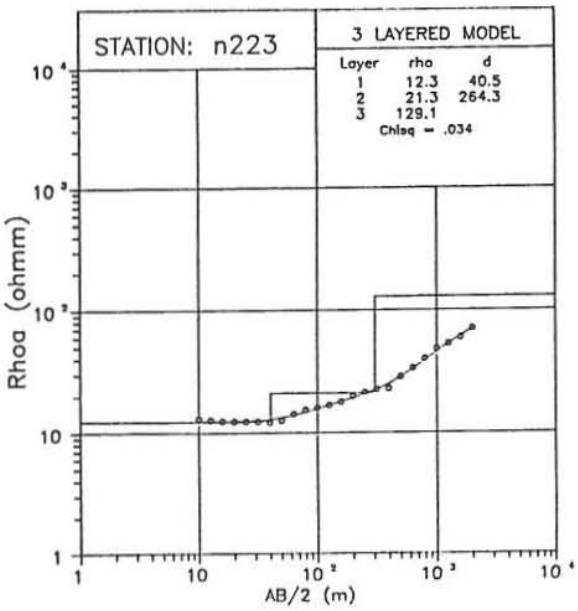
STATION: n223
3 LAYERED MODEL
Layer rho d
1 12.3 40.5
2 21.3 264.3
3 129.1
Chisq = .034
Rhoa (ohmm)
AB/2 (m)

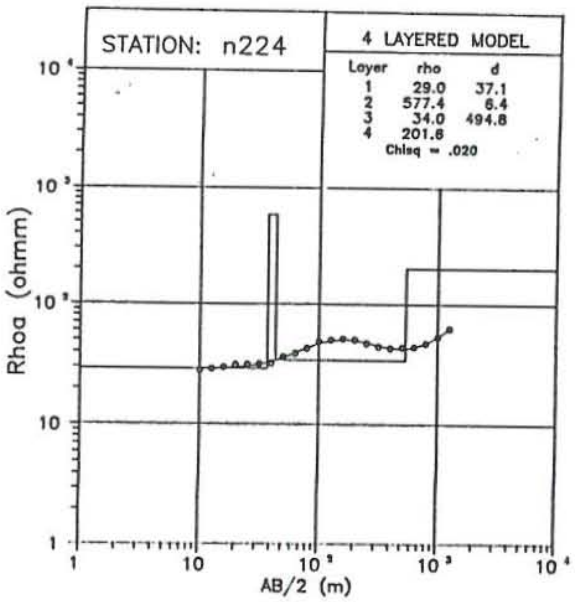
STATION: n224
4 LAYERED MODEL
Layer rho d
1 29.0 37.1
2 577.4 6.4
3 34.0 494.8
4 201.6
Chisq = .020
Rhoa (ohmm)
AB/2 (m)

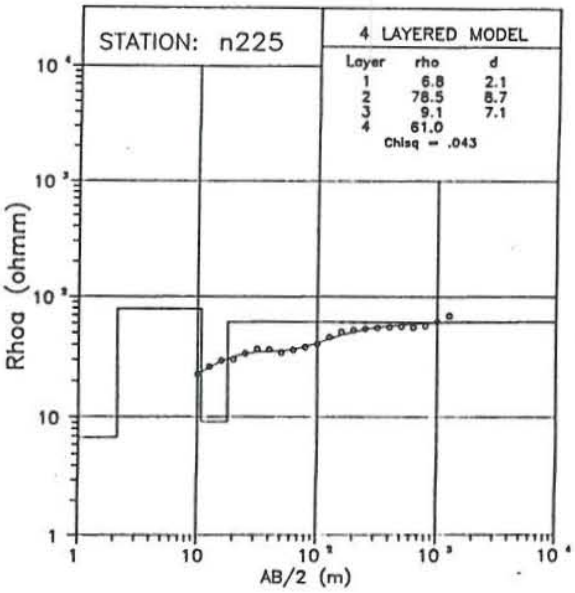
STATION: n225
4 LAYERED MODEL
Layer rho d
1 6.8 2.1
2 78.5 8.7
3 9.1 7.1
4 61.0
Chisq = .043
Rhoa (ohmm)
AB/2 (m)

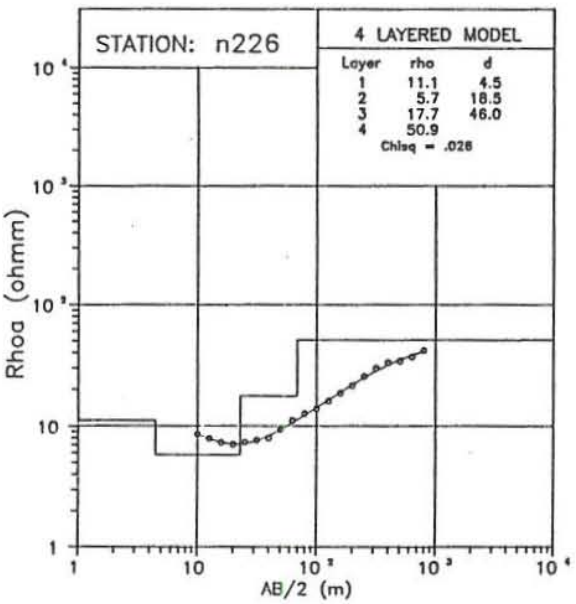
STATION: n226
4 LAYERED MODEL
Layer rho d
1 11.1 4.5
2 5.7 18.5
3 17.7 46.0
4 50.9
Chisq = .026
Rhoa (ohmm)
AB/2 (m)

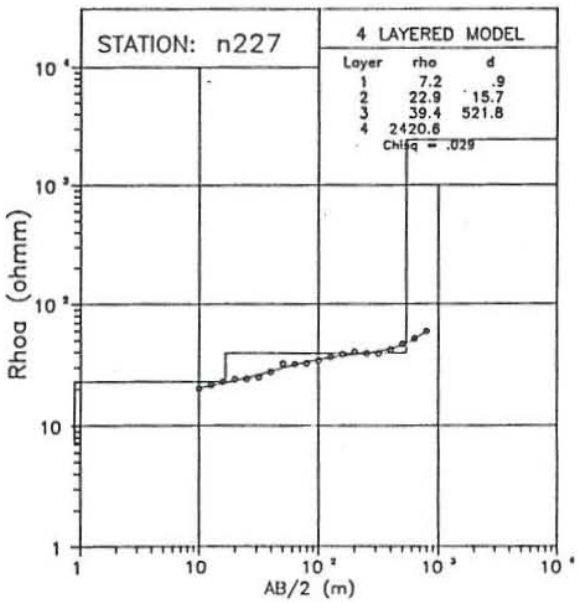
STATION: n227
4 LAYERED MODEL
Layer rho d
1 7.2 .9
2 22.9 15.7
3 39.4 521.8
4 2420.6
Chisq = .029
Rhoa (ohmm)
AB/2 (m)

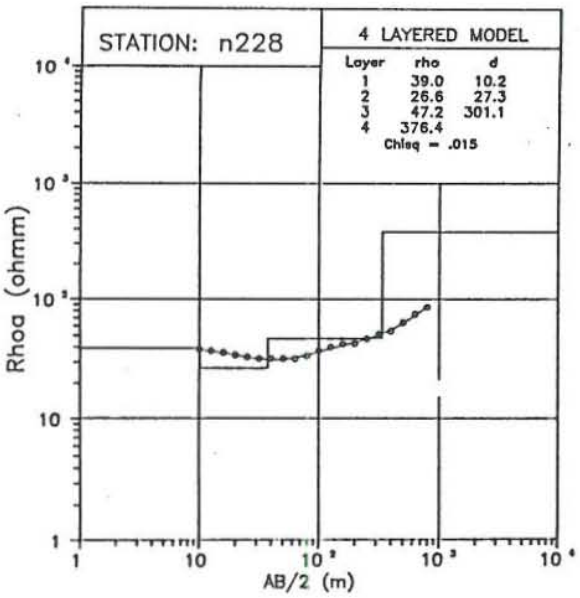
STATION: n228
4 LAYERED MODEL
Layer rho d
1 39.0 10.2
2 26.6 27.3
3 47.2 301.1
4 376.4
Chisq = .015
Rhoa (ohmm)
AB/2 (m)

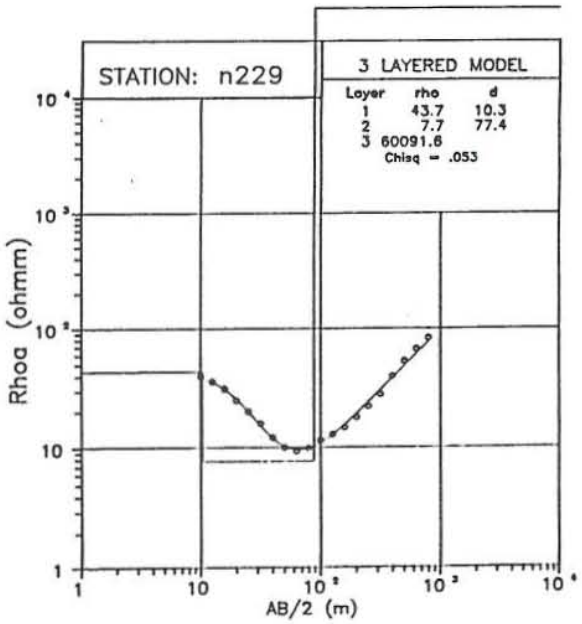
STATION: n229
3 LAYERED MODEL
Layer rho d
1 43.7 10.3
2 7.7 77.4
3 60091.6
Chisq = .053
Rhoa (ohmm)
AB/2 (m)

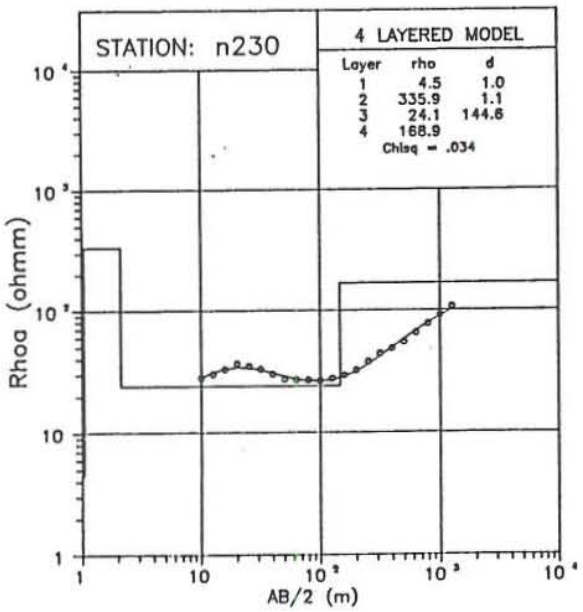
STATION: n230
4 LAYERED MODEL
Layer rho d
1 4.5 1.0
2 335.9 1.1
3 24.1 144.6
4 168.9
Chisq = .034
Rhoa (ohmm)
AB/2 (m)

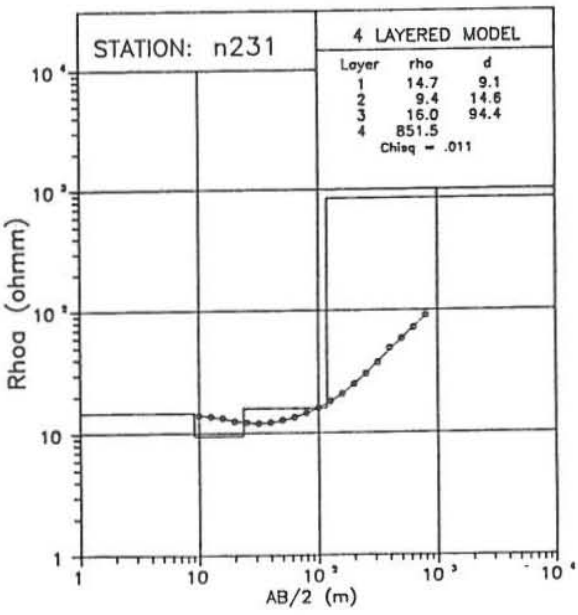
STATION: n231
4 LAYERED MODEL
Layer rho d
1 14.7 9.1
2 9.4 14.6
3 16.0 94.4
4 851.5
Chisq = .011
Rhoa (ohmm)
AB/2 (m)

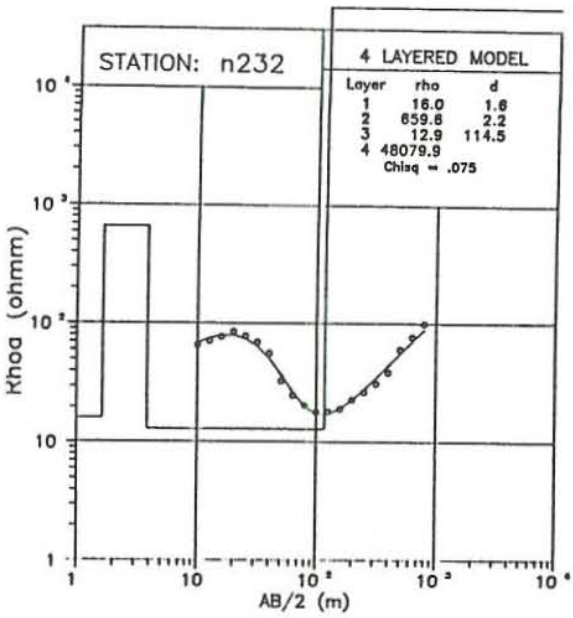
STATION: n232
4 LAYERED MODEL
Layer rho d
1 16.0 1.6
2 659.6 2.2
3 12.9 114.5
4 48079.9
Chisq = .075
Rhoa (ohmm)
AB/2 (m)

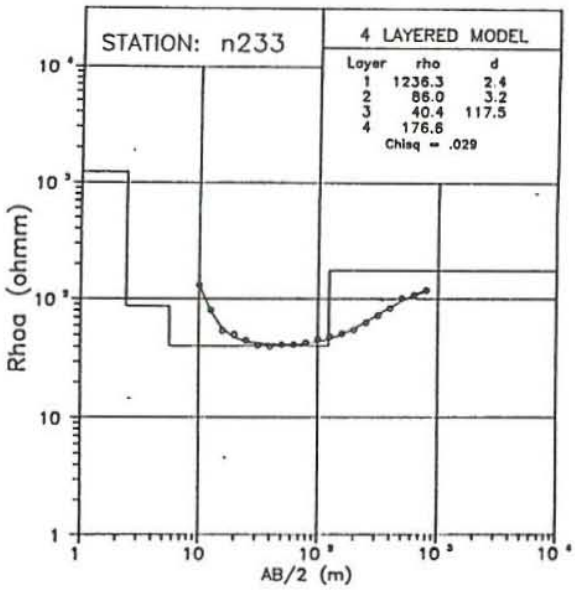
STATION: n233
4 LAYERED MODEL
Layer rho d
1 1236.3 2.4
2 86.0 3.2
3 40.4 117.5
4 176.6
Chisq = .029
Rhoa (ohmm)
AB/2 (m)

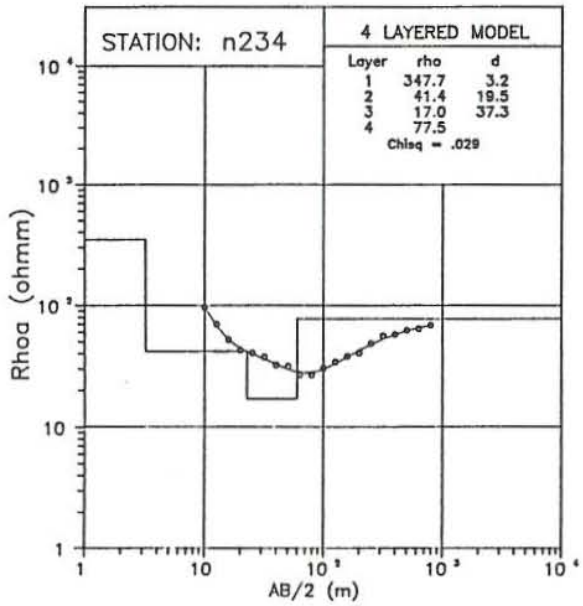
STATION: n234
4 LAYERED MODEL
Layer rho d
1 347.7 3.2
2 41.4 19.5
3 17.0 37.3
4 77.5
Chisq = .029
Rhoa (ohmm)
AB/2 (m)

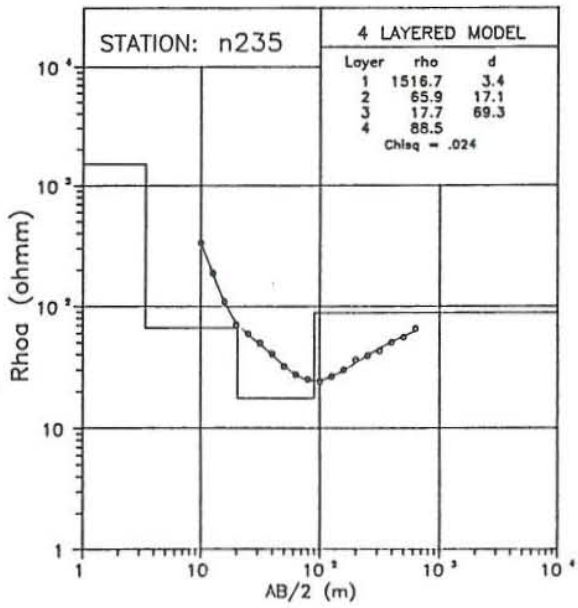
STATION: n235
4 LAYERED MODEL
Layer rho d
1 1516.7 3.4
2 65.9 17.1
3 17.7 69.3
4 88.5
Chisq = .024
Rhoa (ohmm)
AB/2 (m)

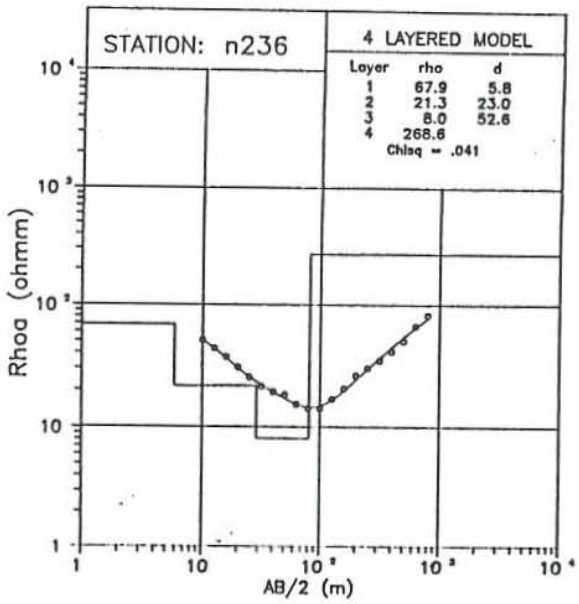
STATION: n236
4 LAYERED MODEL
Layer rho d
1 67.9 5.8
2 21.3 23.0
3 8.0 52.6
4 268.6
Chisq = .041
Rhoa (ohmm)
AB/2 (m)

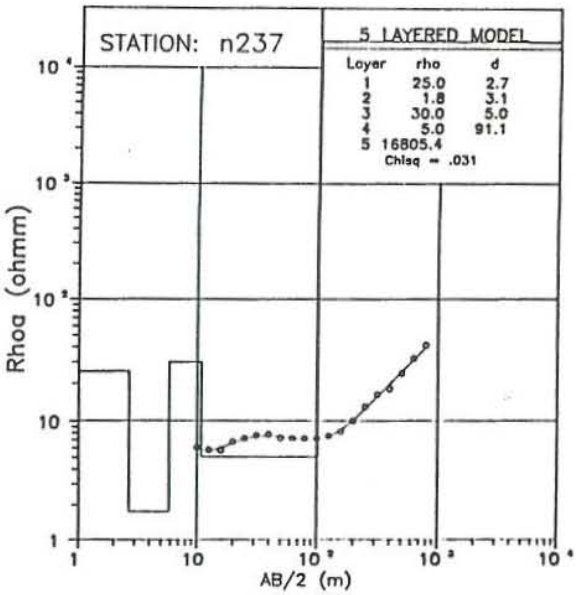
STATION: n237
5 LAYERED MODEL
Layer rho d
1 25.0 2.7
2 1.8 3.1
3 30.0 5.0
4 5.0 91.1
5 16805.4
Chisq = .031
Rhoa (ohmm)
AB/2 (m)

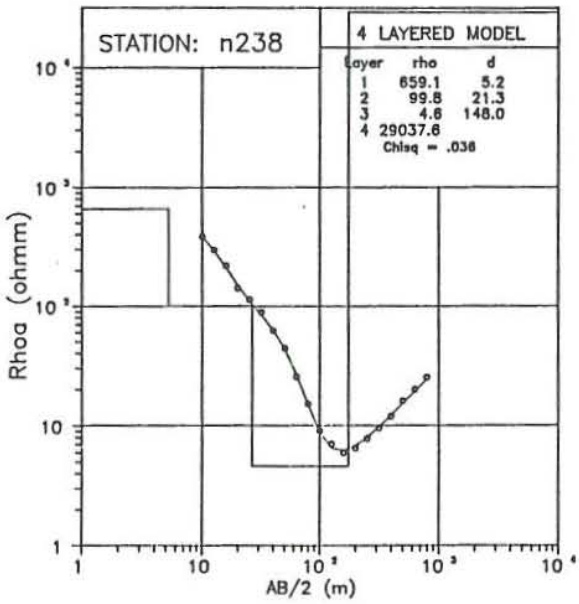
STATION: n238
4 LAYERED MODEL
Layer rho d
1 659.1 5.2
2 99.8 21.3
3 4.6 148.0
4 29037.6
Chisq = .036
Rhoa (ohmm)
AB/2 (m)

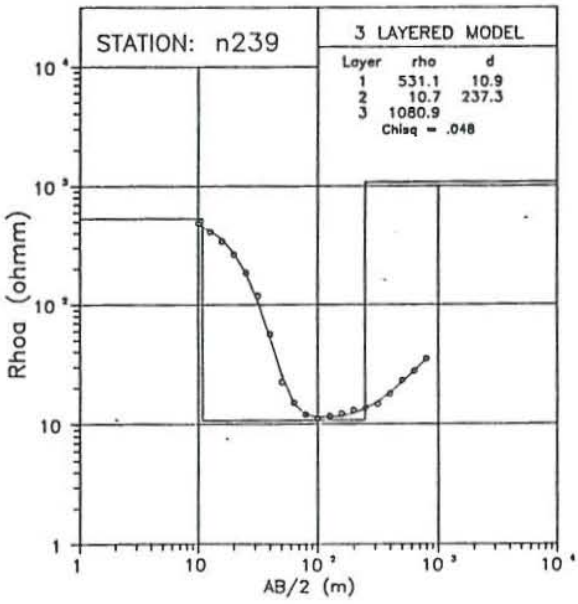
STATION: n239
3 LAYERED MODEL
Layer rho d
1 531.1 10.9
2 10.7 237.3
3 1080.9
Chisq = .048
Rhoa (ohmm)
AB/2 (m)

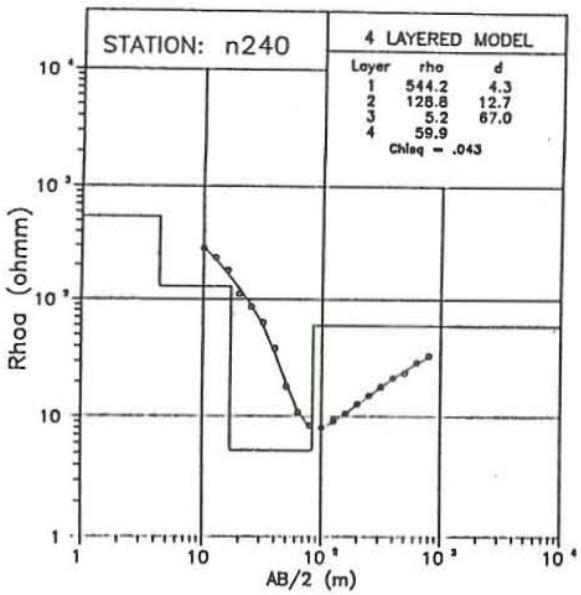
STATION: n240
4 LAYERED MODEL
Layer rho d
1 544.2 4.3
2 128.8 12.7
3 5.2 67.0
4 59.9
Chisq = .043
Rhoa (ohmm)
AB/2 (m)

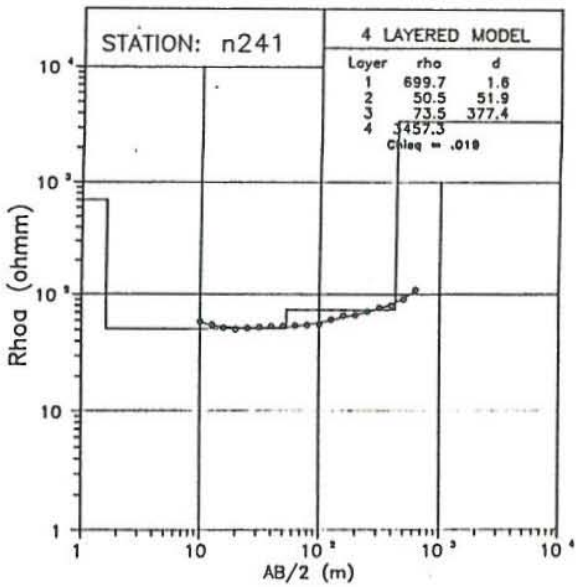
STATION: n241
4 LAYERED MODEL
Layer rho d
1 699.7 1.6
2 50.5 51.9
3 73.5 377.4
4 3457.3
Chisq = .018
Rhoa (ohmm)
AB/2 (m)

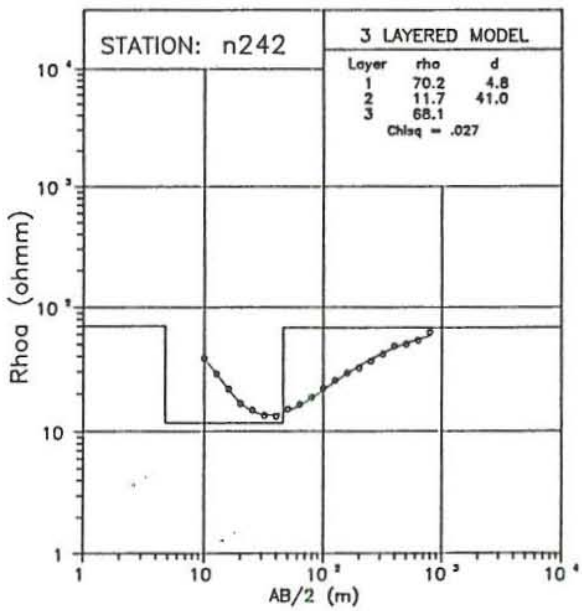
STATION: n242
3 LAYERED MODEL
Layer rho d
1 70.2 4.8
2 11.7 41.0
3 68.1
Chisq = .027
Rhoa (ohmm)
AB/2 (m)

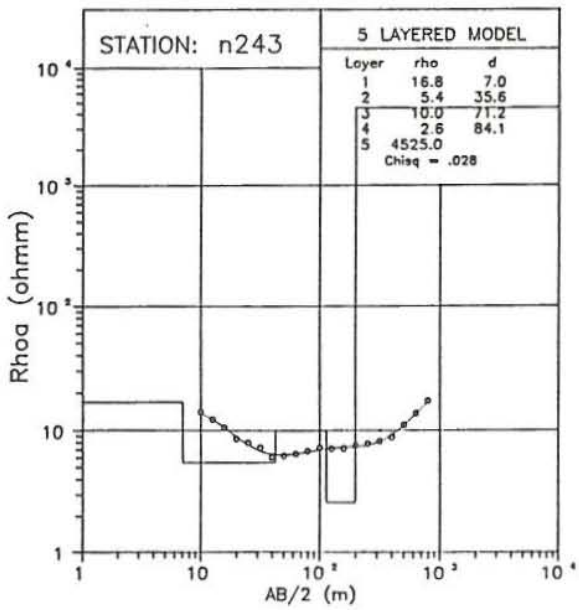
STATION: n243
5 LAYERED MODEL
Layer rho d
1 16.8 7.0
2 5.4 35.6
3 10.0 71.2
4 2.6 84.1
5 4525.0
Chisq = .028
Rhoa (ohmm)
AB/2 (m)

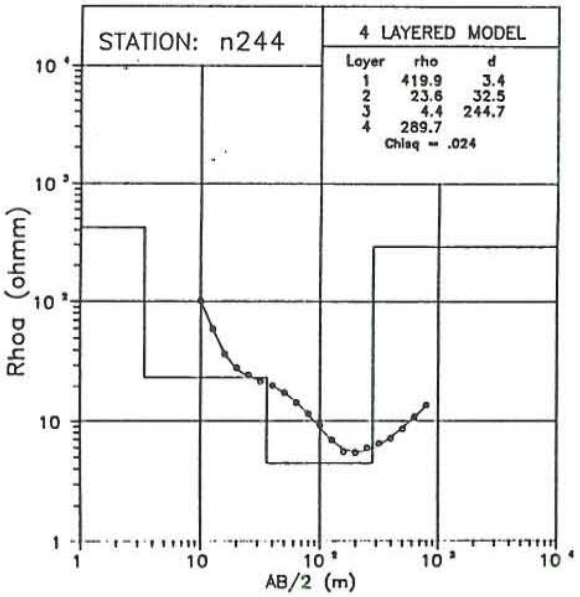
STATION: n244
4 LAYERED MODEL
Layer rho d
1 419.9 3.4
2 23.6 32.5
3 4.4 244.7
4 289.7
Chisq = .024
Rhoa (ohmm)
AB/2 (m)

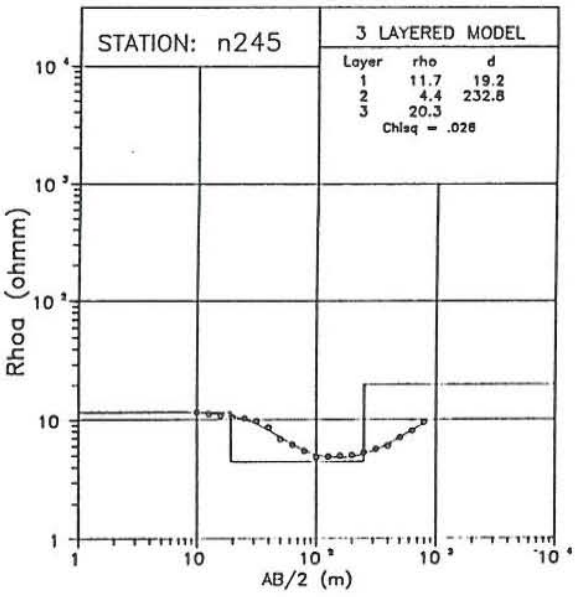
STATION: n245
3 LAYERED MODEL
Layer rho d
1 11.7 19.2
2 4.4 232.8
3 20.3
Chisq = .026
Rhoa (ohmm)
AB/2 (m)

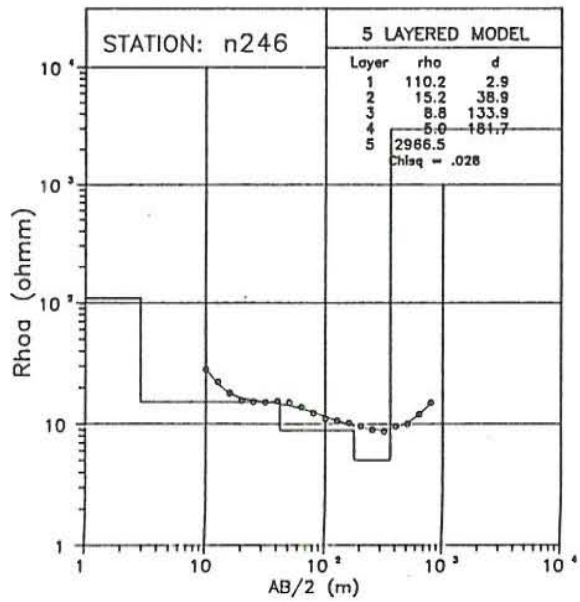
STATION: n246
5 LAYERED MODEL
Layer rho d
1 110.2 2.9
2 15.2 38.9
3 8.8 133.9
4 5.0 181.7
5 2966.5
Chisq = .028
Rhoa (ohmm)
AB/2 (m)

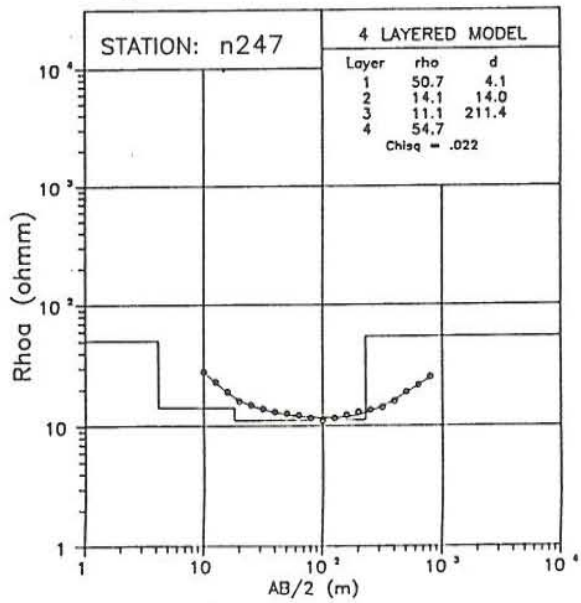
STATION: n247
4 LAYERED MODEL
Layer rho d
1 50.7 4.1
2 14.1 14.0
3 11.1 211.4
4 54.7
Chisq = .022
Rhoa (ohmm)
AB/2 (m)

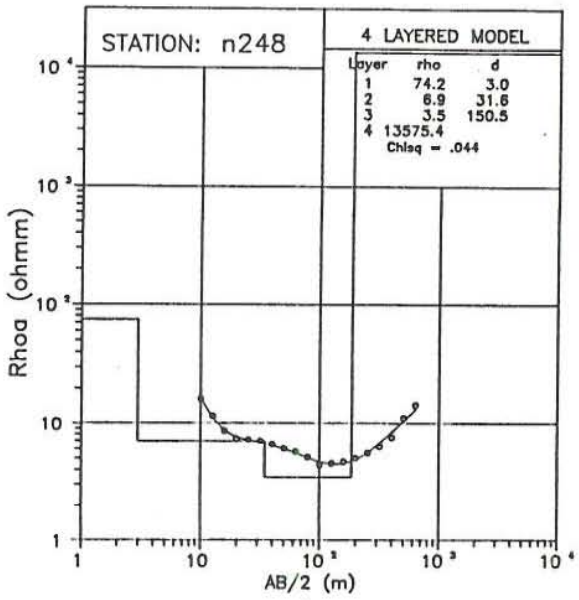
STATION: n248
4 LAYERED MODEL
Layer rho d
1 74.2 3.0
2 6.9 31.6
3 3.5 150.5
4 13575.4
Chisq = .044
Rhoa (ohmm)
AB/2 (m)

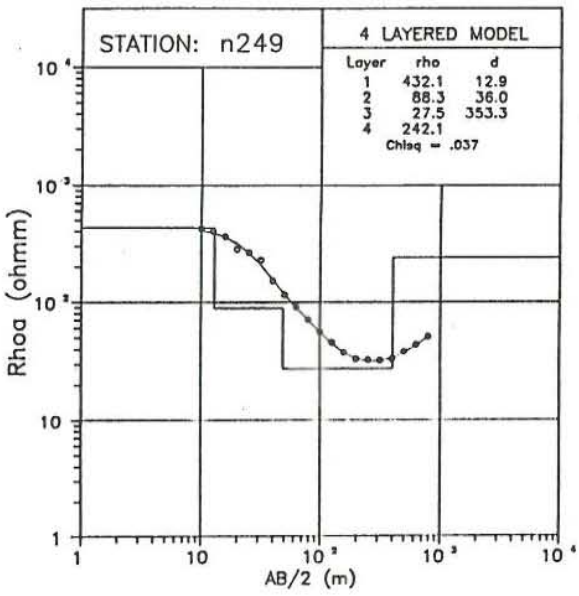
STATION: n249
4 LAYERED MODEL
Layer rho d
1 432.1 12.9
2 88.3 36.0
3 27.5 353.3
4 242.1
Chisq = .037
Rhoa (ohmm)
AB/2 (m)

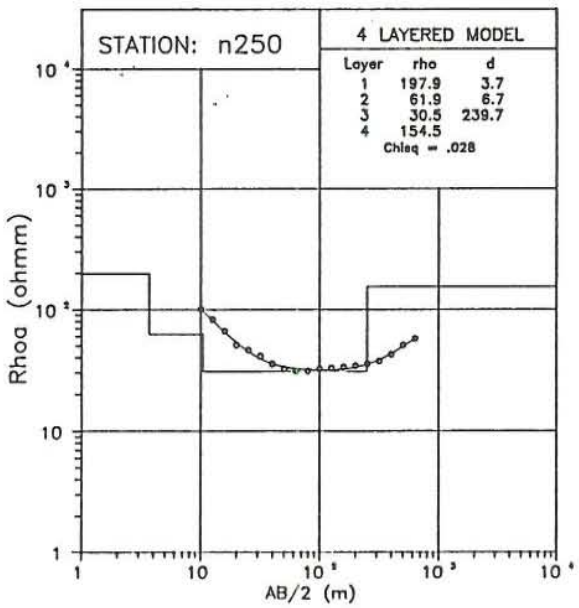
STATION: n250
4 LAYERED MODEL
Layer rho d
1 197.9 3.7
2 61.9 6.7
3 30.5 239.7
4 154.5
Chisq = .028
Rhoa (ohmm)
AB/2 (m)

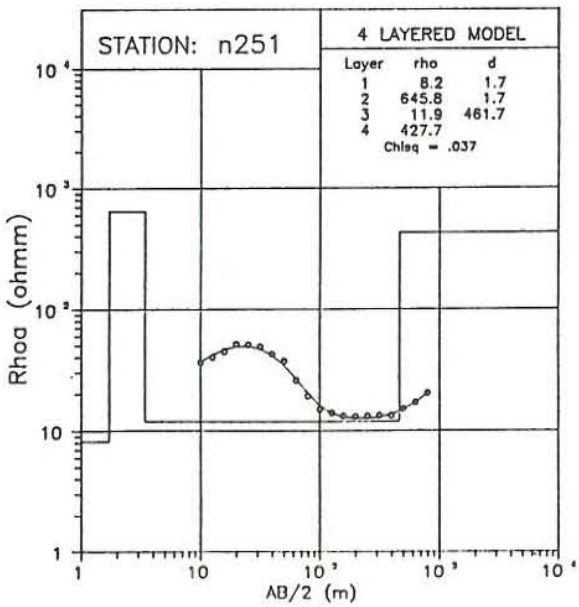
STATION: n251
4 LAYERED MODEL
Layer rho d
1 8.2 1.7
2 645.8 1.7
3 11.9 461.7
4 427.7
Chisq = .037
Rhoa (ohmm)
AB/2 (m)

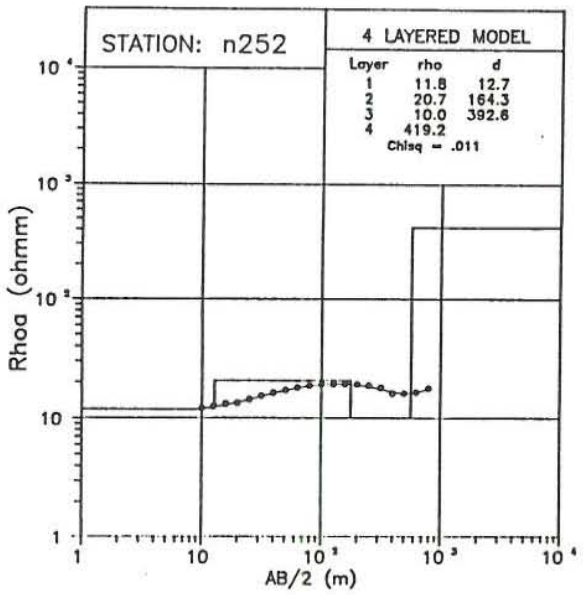
STATION: n252
4 LAYERED MODEL
Layer rho d
1 11.8 12.7
2 20.7 164.3
3 10.0 392.6
4 419.2
Chisq = .011
Rhoa (ohmm)
AB/2 (m)

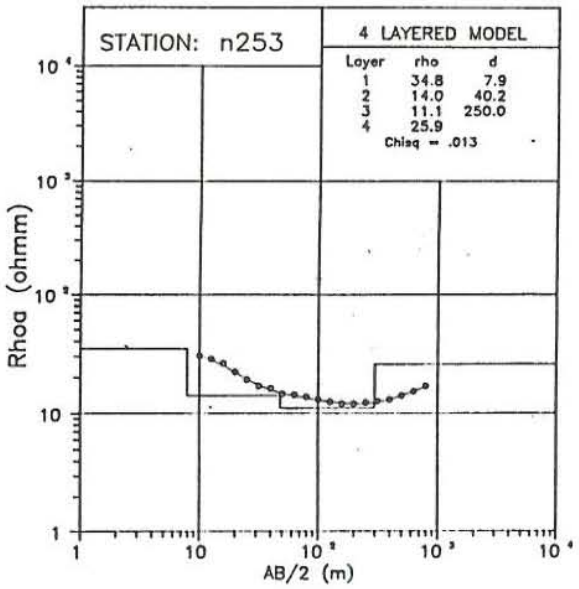
STATION: n253
4 LAYERED MODEL
Layer rho d
1 34.8 7.9
2 14.0 40.2
3 11.1 250.0
4 25.9
Chisq = .013
Rhoa (ohmm)
AB/2 (m)

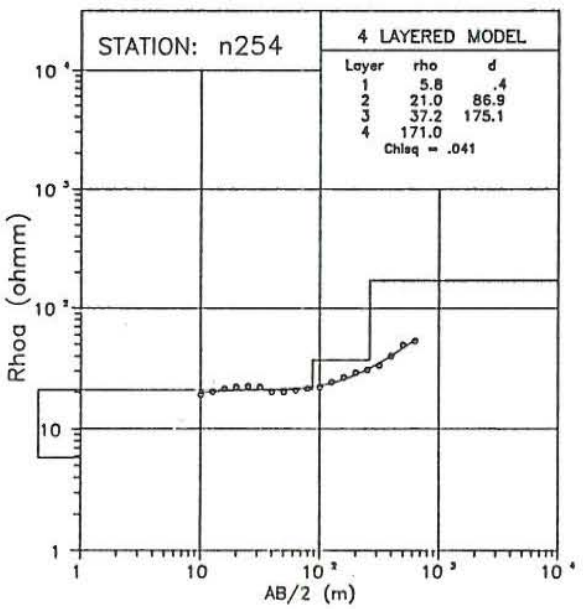
STATION: n254
4 LAYERED MODEL
Layer rho d
1 5.8 .4
2 21.0 86.9
3 37.2 175.1
4 171.0
Chisq = .041
Rhoa (ohmm)
AB/2 (m)

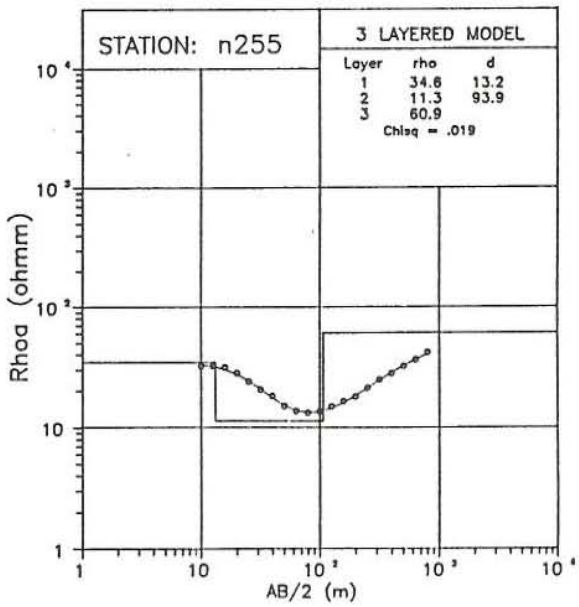
STATION: n255
3 LAYERED MODEL
Layer rho d
1 34.6 13.2
2 11.3 93.9
3 60.9
Chisq = .019
Rhoa (ohmm)
AB/2 (m)

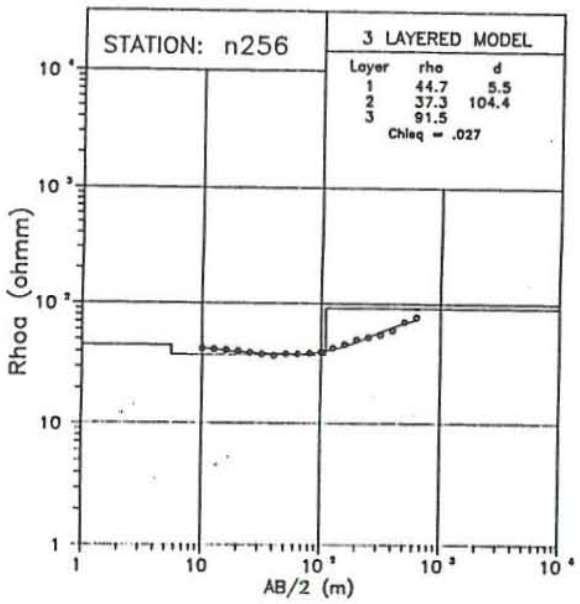
STATION: n256
3 LAYERED MODEL
Layer rho d
1 44.7 5.5
2 37.3 104.4
3 91.5
Chisq = .027
Rhoa (ohmm)
AB/2 (m)

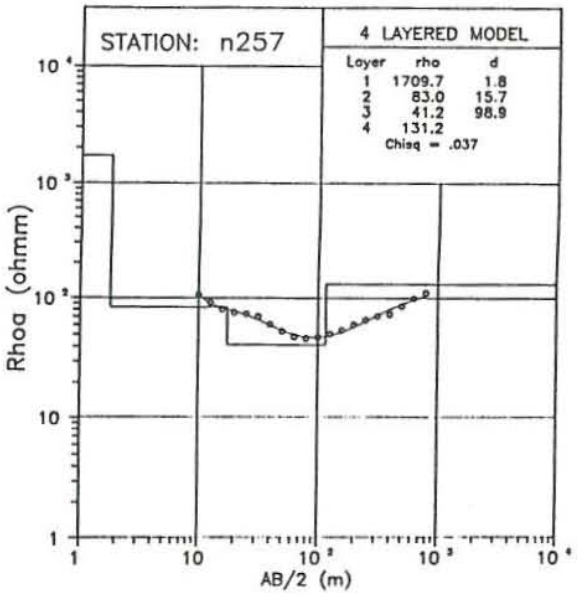
STATION: n257
4 LAYERED MODEL
Layer rho d
1 1709.7 1.8
2 83.0 15.7
3 41.2 98.9
4 131.2
Chisq = .037
Rhoa (ohmm)
AB/2 (m)

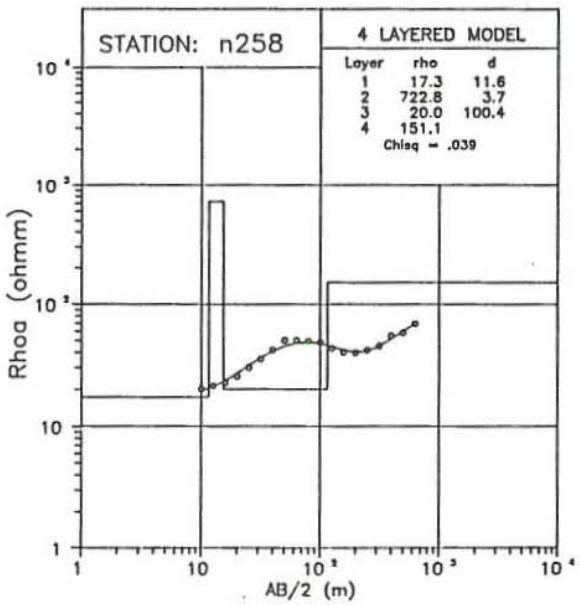
STATION: n258
4 LAYERED MODEL
Layer rho d
1 17.3 11.6
2 722.8 3.7
3 20.0 100.4
4 151.1
Chisq = .039
Rhoa (ohmm)
AB/2 (m)

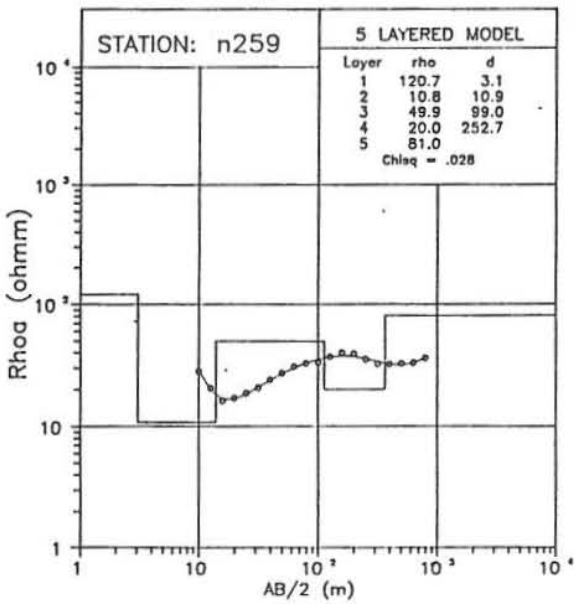
STATION: n259
5 LAYERED MODEL
Layer rho d
1 120.7 3.1
2 10.8 10.9
3 49.9 99.0
4 20.0 252.7
5 81.0
Chisq = .028
Rhoa (ohmm)
AB/2 (m)

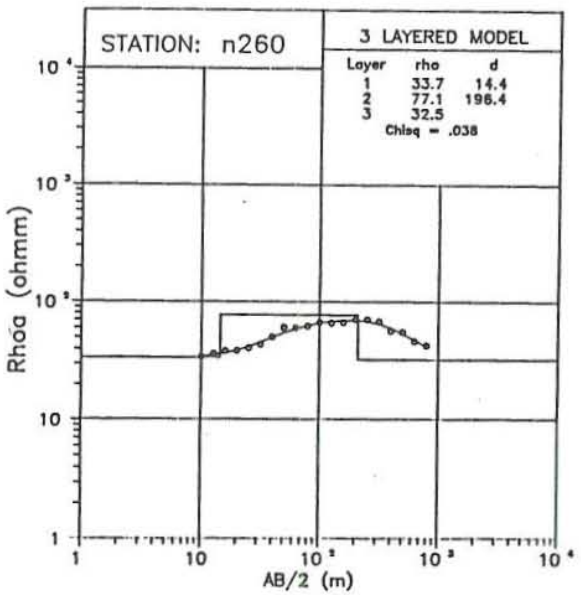
STATION: n260
3 LAYERED MODEL
Layer rho d
1 33.7 14.4
2 77.1 196.4
3 32.5
Chisq = .038
Rhoa (ohmm)
AB/2 (m)

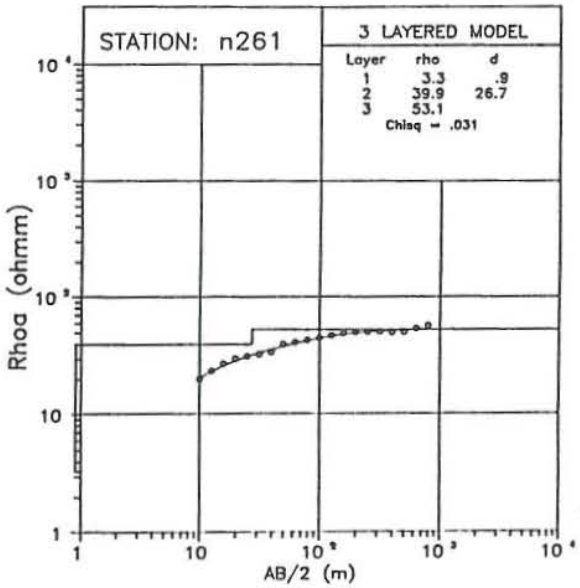
STATION: n261
3 LAYERED MODEL
Layer rho d
1 3.3 .9
2 39.9 26.7
3 53.1
Chisq = .031
Rhoa (ohmm)
AB/2 (m)

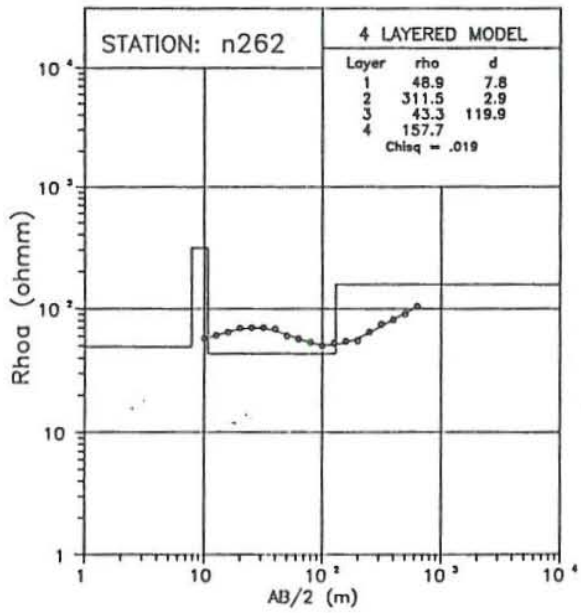
STATION: n262
4 LAYERED MODEL
Layer rho d
1 48.9 7.8
2 311.5 2.9
3 43.3 119.9
4 157.7
Chisq = .019
Rhoa (ohmm)
AB/2 (m)

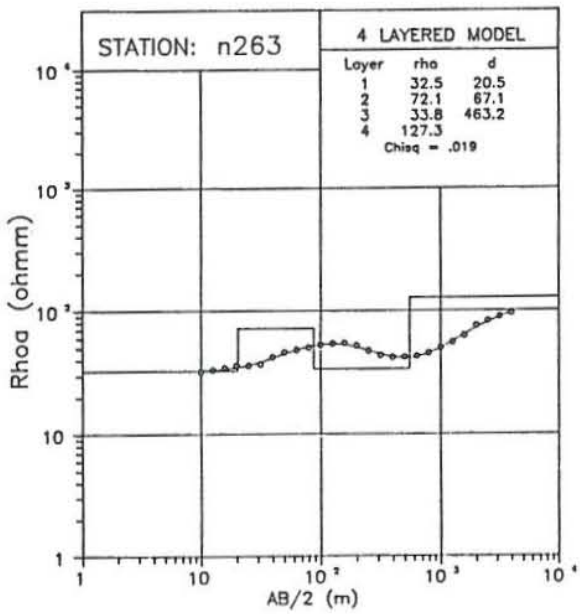
STATION: n263
4 LAYERED MODEL
Layer rho d
1 32.5 20.5
2 72.1 67.1
3 33.8 463.2
4 127.3
Chisq = .019
Rhoa (ohmm)
AB/2 (m)

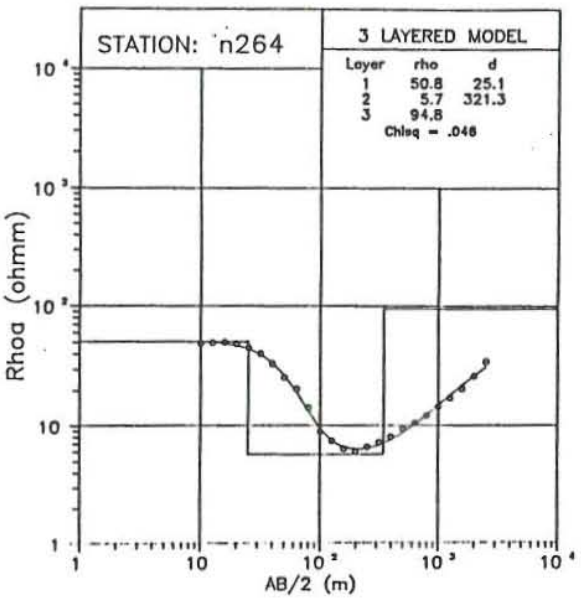
STATION: n264
3 LAYERED MODEL
Layer rho d
1 50.8 25.1
2 5.7 321.3
3 94.8
Chisq = .046
Rhoa (ohmm)
AB/2 (m)

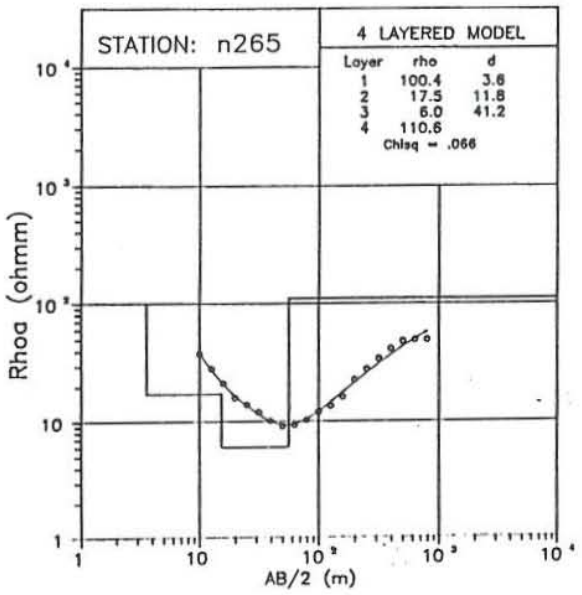
STATION: n265
4 LAYERED MODEL
Layer rho d
1 100.4 3.6
2 17.5 11.8
3 6.0 41.2
4 110.6
Chisq = .066
Rhoa (ohmm)
AB/2 (m)

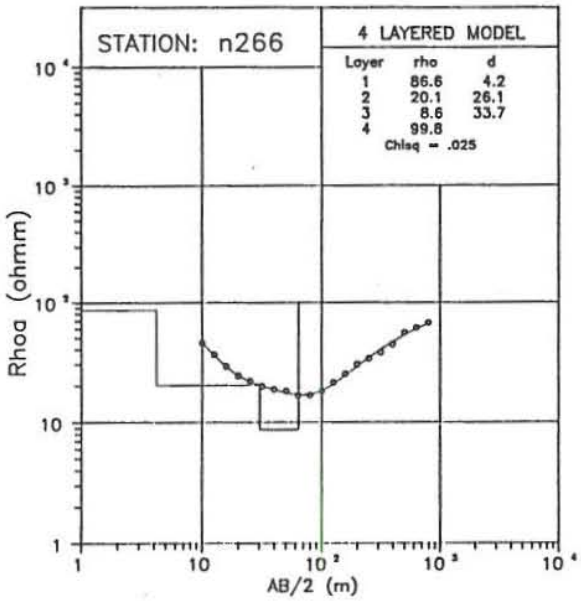
STATION: n266
4 LAYERED MODEL
Layer rho d
1 86.6 4.2
2 20.1 26.1
3 8.6 33.7
4 99.8
Chisq = .025
Rhoa (ohmm)
AB/2 (m)

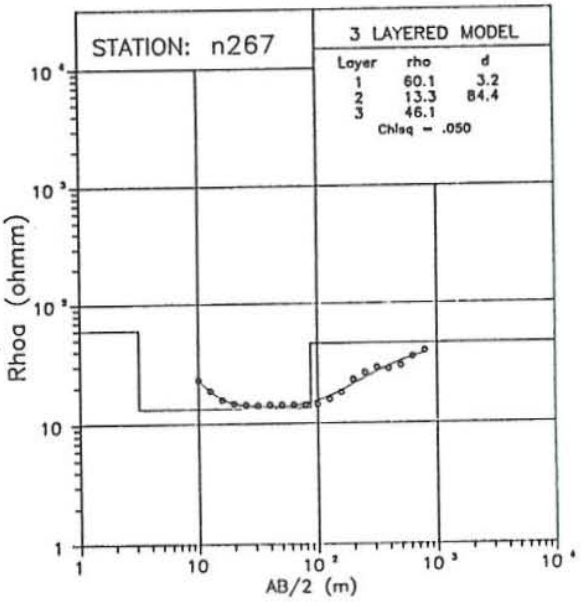
STATION: n267
3 LAYERED MODEL
Layer rho d
1 60.1 3.2
2 13.3 84.4
3 46.1
Chisq = .050
Rhoa (ohmm)
AB/2 (m)

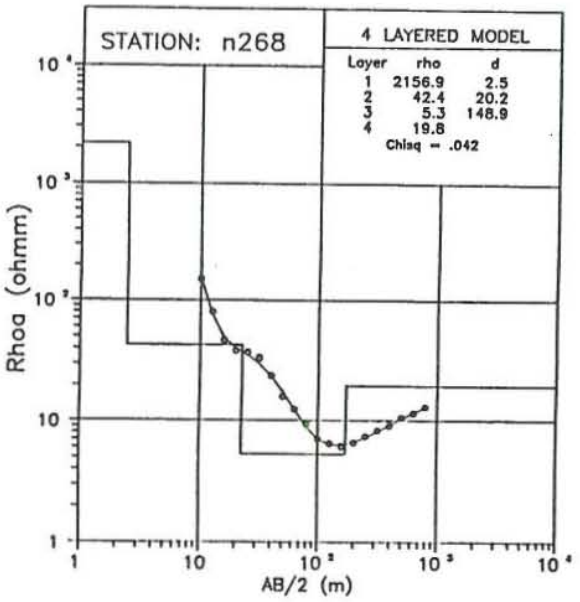
STATION: n268
4 LAYERED MODEL
Layer rho d
1 2156.9 2.5
2 42.4 20.2
3 5.3 148.9
4 19.8
Chisq = .042
Rhoa (ohmm)
AB/2 (m)

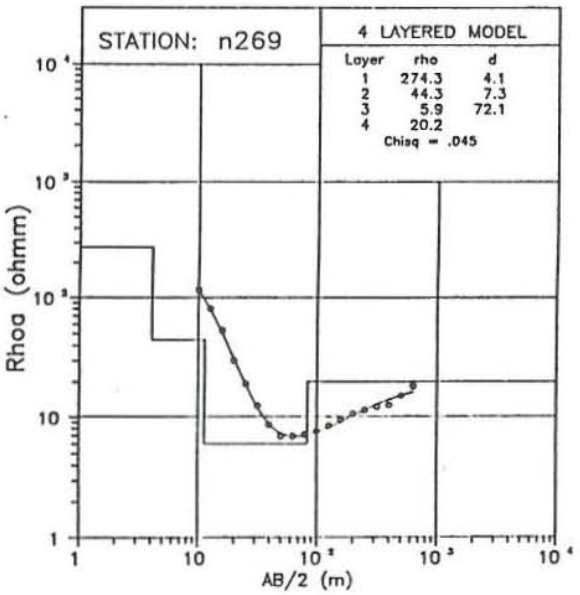
STATION: n269
4 LAYERED MODEL
Layer rho d
1 274.3 4.1
2 44.3 7.3
3 5.9 72.1
4 20.2
Chisq = .045
Rhoa (ohmm)
AB/2 (m)

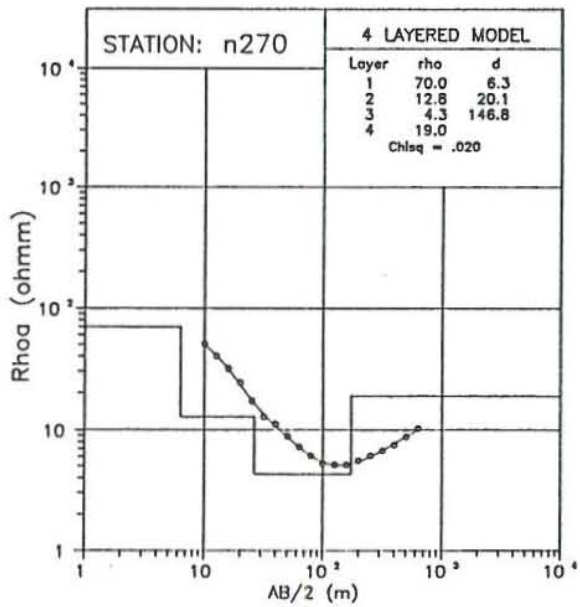
STATION: n270
4 LAYERED MODEL
Layer rho d
1 70.0 6.3
2 12.8 20.1
3 4.3 146.8
4 19.0
Chisq = .020
Rhoa (ohmm)
AB/2 (m)

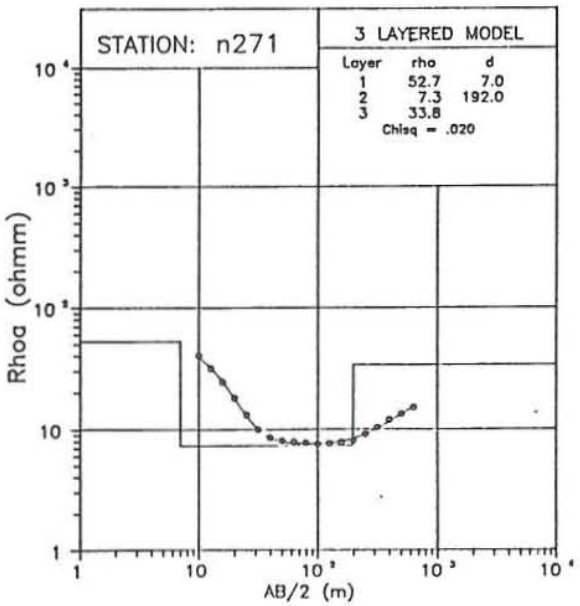
STATION: n271
3 LAYERED MODEL
Layer rho d
1 52.7 7.0
2 7.3 192.0
3 33.8
Chisq = .020
Rhoa (ohmm)
AB/2 (m)

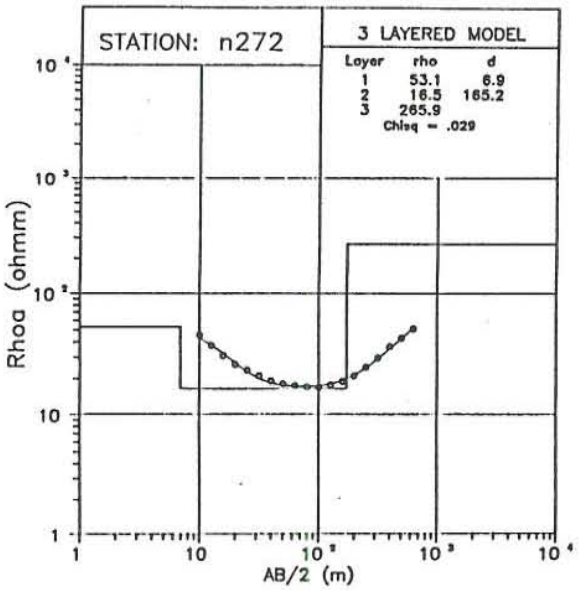
STATION: n272
3 LAYERED MODEL
Layer rho d
1 53.1 6.9
2 16.5 165.2
3 265.9
Chisq = .029
Rhoa (ohmm)
AB/2 (m)

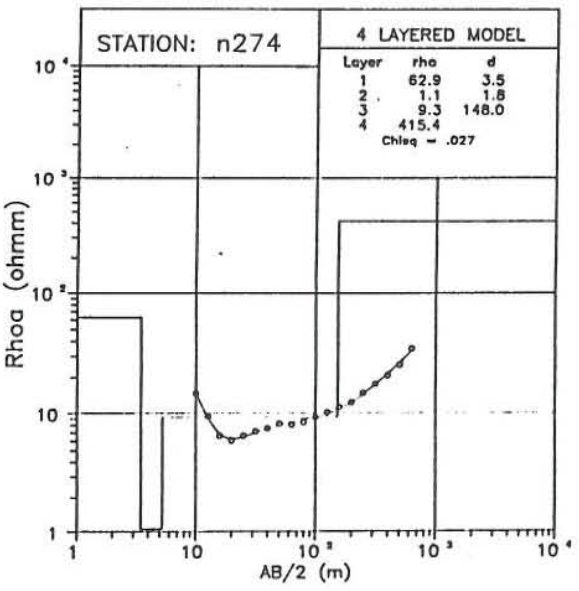
STATION: n274
4 LAYERED MODEL
Layer rho d
1 62.9 3.5
2 1.1 1.8
3 9.3 148.0
4 415.4
Chisq = .027
Rhoa (ohmm)
AB/2 (m)

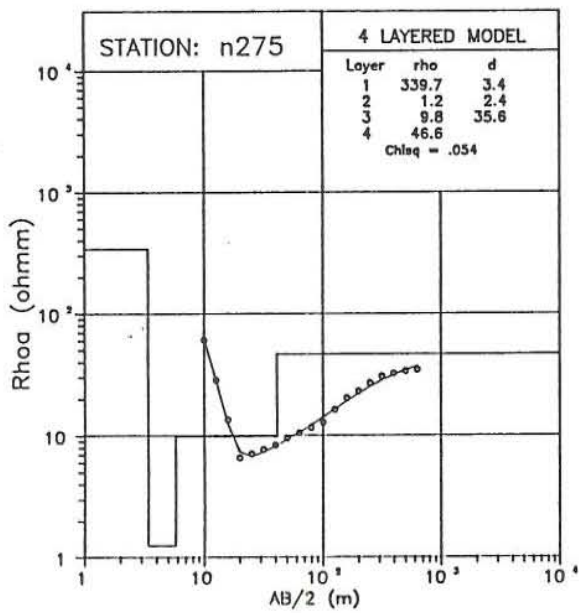
STATION: n275
4 LAYERED MODEL
Layer rho d
1 339.7 3.4
2 1.2 2.4
3 9.8 35.6
4 46.6
Chisq = .054
Rhoa (ohmm)
AB/2 (m)

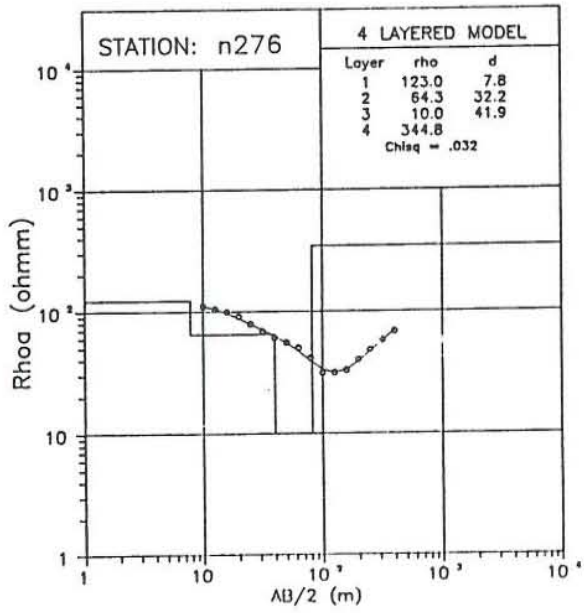
STATION: n276
4 LAYERED MODEL
Layer rho d
1 123.0 7.8
2 64.3 32.2
3 10.0 41.9
4 344.8
Chisq = .032
Rhoa (ohmm)
AB/2 (m)

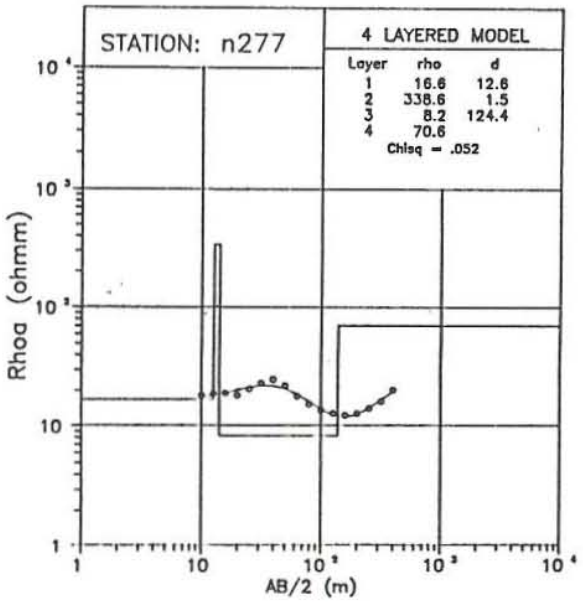
STATION: n277
4 LAYERED MODEL
Layer rho d
1 16.6 12.6
2 338.6 1.5
3 8.2 124.4
4 70.6
Chisq = .052
Rhoa (ohmm)
AB/2 (m)

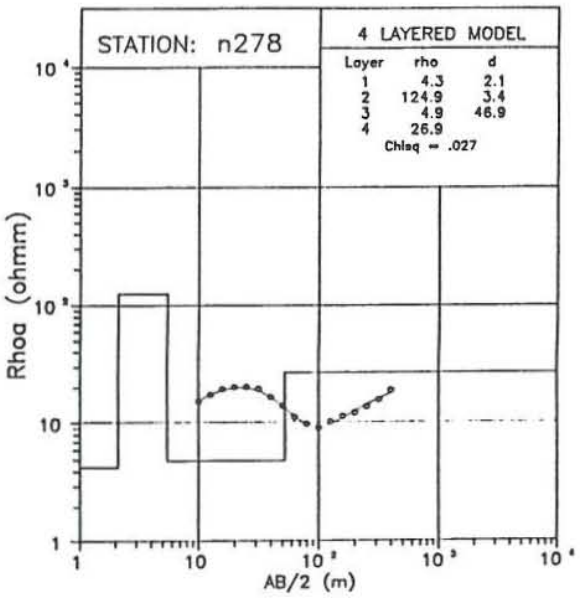
STATION: n278
4 LAYERED MODEL
Layer rho d
1 4.3 2.1
2 124.9 3.4
3 4.9 46.9
4 26.9
Chisq = .027
Rhoa (ohmm)
AB/2 (m)

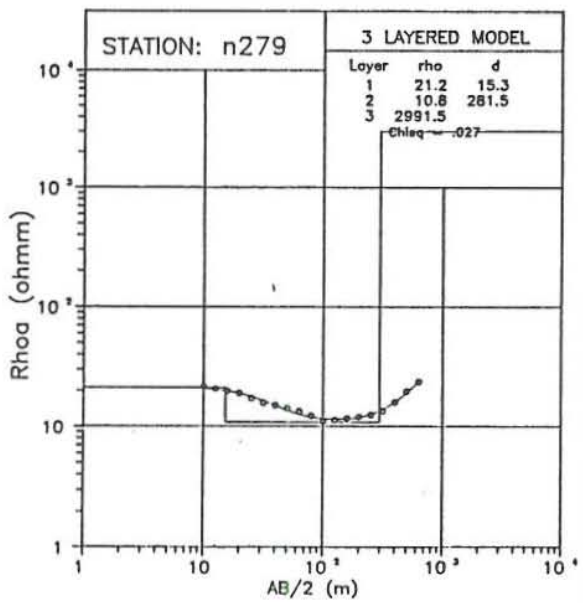
STATION: n279
3 LAYERED MODEL
Layer rho d
1 21.2 15.3
2 10.8 281.5
3 2991.5
Chisq = .027
Rhoa (ohmm)
AB/2 (m)

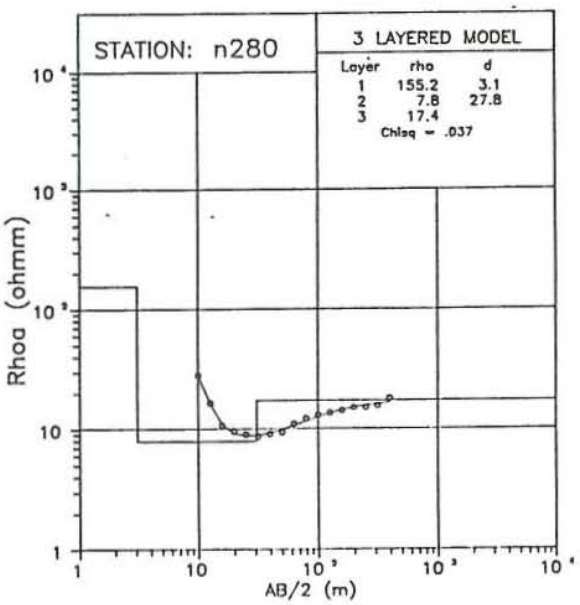
STATION: n280
3 LAYERED MODEL
Layer rho d
1 155.2 3.1
2 7.8 27.8
3 17.4
Chisq = .037
Rhoa (ohmm)
AB/2 (m)

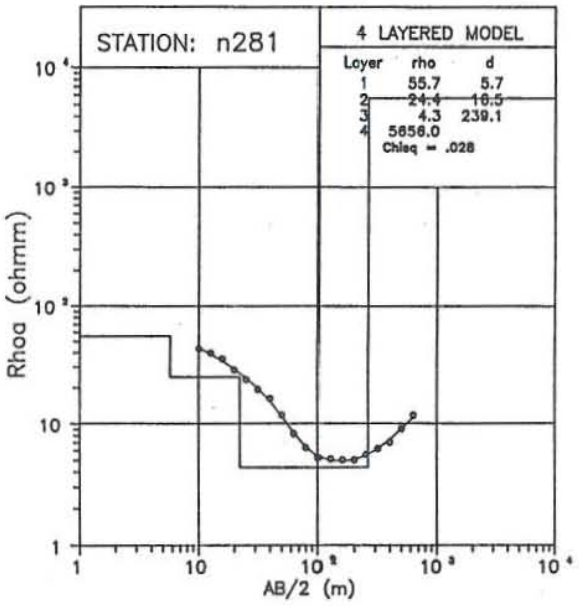
STATION: n281
4 LAYERED MODEL
Layer rho d
1 55.7 5.7
2 24.4 18.5
4.3 239.1
5656.0
Chisq = .028
Rhoa (ohmm)
AB/2 (m)

APPENDIX II

Two-dimensional interpretation
of Schlumberger soundings:

Measured apparent resistivity curves (shown as points) and calculated apparent resistivity curves (shown as continuous curves). The two-dimensional model is shown in Figure 18

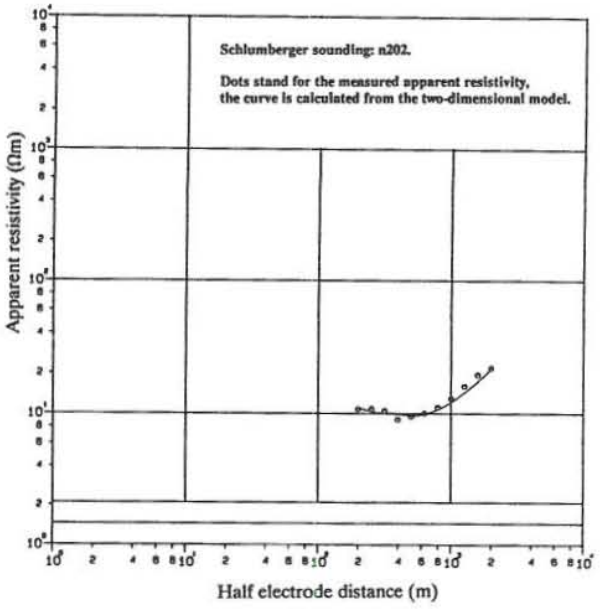
Schlumberger sounding: n202.
Dots stand for the measured apparent resistivity,
the curve is calculated from the two-dimensional model.
Apparent resistivity (Ωm)
Half electrode distance (m)

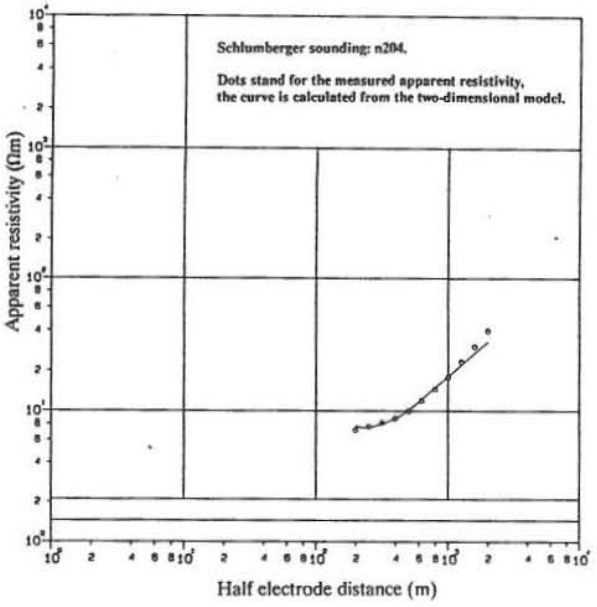
Schlumberger sounding: n204.
Dots stand for the measured apparent resistivity,
the curve is calculated from the two-dimensional model.
Apparent resistivity (Ωm)
Half electrode distance (m)

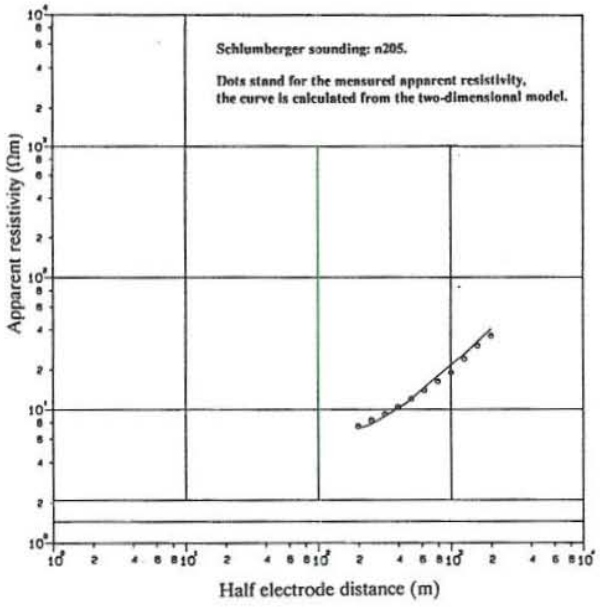
Schlumberger sounding: n205.
Dots stand for the measured apparent resistivity,
the curve is calculated from the two-dimensional model.
Apparent resistivity (Ωm)
Half electrode distance (m)

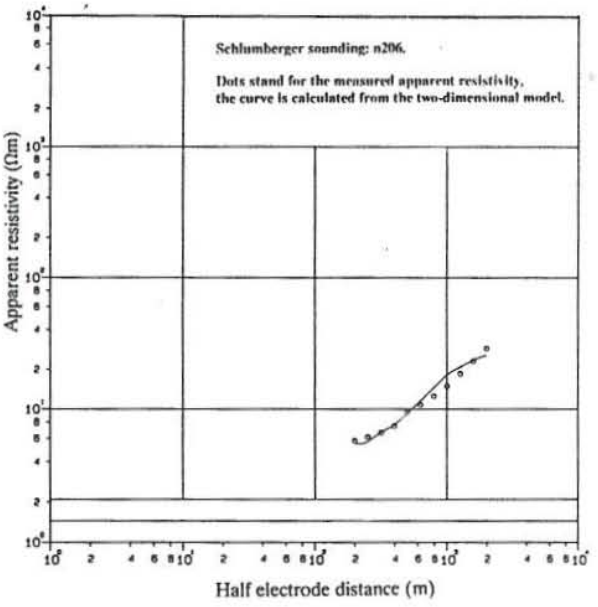
Schlumberger sounding: n206.
Dots stand for the measured apparent resistivity,
the curve is calculated from the two-dimensional model.
Apparent resistivity (Ωm)
Half electrode distance (m)

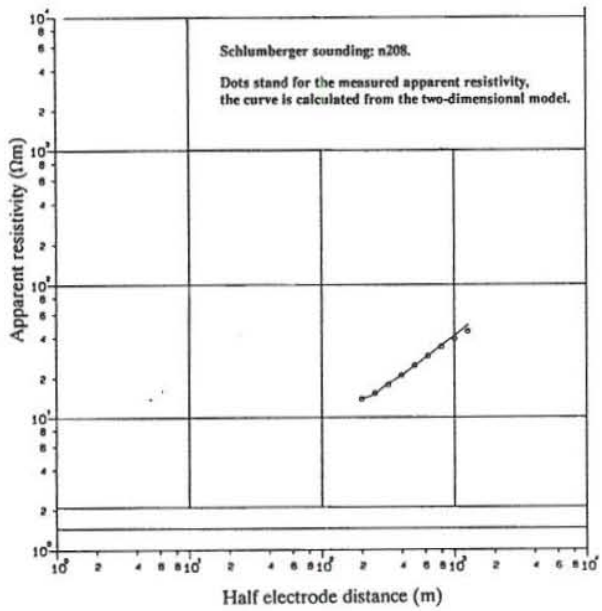
Schlumberger sounding: n208.
Dots stand for the measured apparent resistivity,
the curve is calculated from the two-dimensional model.
Apparent resistivity (Ωm)
Half electrode distance (m)